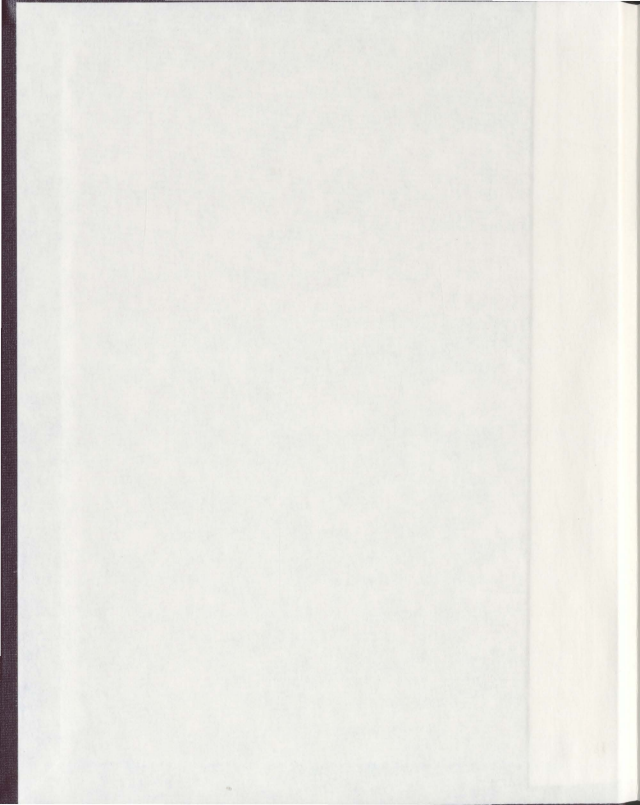


L-TYPE CALCIUM CHANNELS MODULATE FIRING
PATTERNS OF VENTRAL TEGMENTAL AREA NEURONS

ANDREA NICOLE PITTMAN



**L-TYPE CALCIUM CHANNELS MODULATE FIRING
PATTERNS OF VENTRAL TEGMENTAL AREA NEURONS**

by

© Andrea Nicole Pittman

A thesis submitted to the School of Graduate Studies
in partial fulfillment of the requirements for the degree of
Master of Science

Division of Biomedical Sciences
Faculty of Medicine
Memorial University of Newfoundland

September 2012

St. John's

Newfoundland

Abstract

Neurons originating in the ventral tegmental area (VTA) have been implicated in disease states such as drug addiction and schizophrenia. It is believed excessive dopamine transmission (via dopaminergic neuron excitation) underlies both disease states. As dopamine is released because of action potential firing, more intense spiking will result in more neurotransmitter being released. Therefore, understanding the mechanisms modulating firing patterns may lead to a better understanding of such diseases.

This thesis seeks to compare the basic electrophysiological properties of dopaminergic (DAergic) and GABAergic neurons within the VTA, as well as to identify how L-type calcium channels (LTCC) modulate firing patterns of both cell populations. Using a mouse model with green fluorescent protein labeled DAergic neurons, combined with patch clamp recordings, I find two commonly used fingerprinting criteria, I_h current and dopamine autoinhibition, are specific to DAergic neurons. As well, using an LTCC transgenic mouse model and various LTCC modulators, I show LTCC activation modulates burst firing similarly in DAergic and non-DAergic neurons of the VTA. More specifically, the $Ca_v1.3$ subtype is responsible for this LTCC induced bursting.

Understanding the intrinsic modulators of firing pattern regulation in both DAergic and non-DAergic neurons of the VTA can provide a better understanding of disease states associated with dopamine transmission dysregulation, potentially leading to a target for future treatment options.

Acknowledgements

First, I wish to thank my supervisor, Dr Xihua Chen. He willingly accepted me as a Masters student and believed in my research potential, even though I had very little experience in the Neuroscience field. His constant lessons have helped me become a better scientist as well as a better person. I will forever be grateful for all the wisdom he shared with me and the kindness he always showed me.

I wish to thank my supervisory committee members, Drs Jules Doré and John McLean. Their input and support helped make my project and thesis a success.

I also wish to thank all of my family and friends who have provided endless support during my graduate studies. Through the ups and downs they always listened and provided the support I needed. Without them this journey would not have been possible.

List of Abbreviations

ACSF; artificial cerebrospinal fluid
ACh; acetylcholine
AChR; acetylcholine receptor
AHP; afterhyperpolarization
AP; action potential
BFR; basal firing rate
DA; dopamine
DAT; dopamine transporter
EGFP; enhanced green fluorescent protein
GAD; glutamic acid decarboxylase
GABA; γ -aminobutyric acid
HVA; high voltage activated
 I_h ; hyperpolarization activated inward current
ISI; interspike interval
LDTg; laterodorsal tegmental nuclei
LTCC; L-type calcium channel
LVA; low voltage activated
NAc; nucleus accumbens
mGluRs; metabotropic glutamate receptors
PKC; protein kinase C
PKM; protein kinase M
PFC; prefrontal cortex

PPTg; pedunculopontine tegmental nuclei

RMP; resting membrane potential

SEM; standard error of the mean

SK channel; calcium activated small conductance potassium channel

SN; substantia nigra

TH; tyrosine hydroxylase

VTA; ventral tegmental area

WT; wildtype

List of Figures

Figure 1.1	The midbrain DAergic systems	6
Figure 1.2	The connectivity of the VTA	7
Figure 1.3	Firing patterns of midbrain neurons	18
Figure 2.1	Identifying the neurotransmitter content of VTA neurons	45
Figure 2.2	The measurement of afterhyperpolarizations in VTA neurons	47
Figure 3.1	Genotyping results for transgenic mice	52
Figure 3.2	Expression of EGFP in the VTA of the adult transgenic mouse	54
Figure 3.3	DAergic neurons display dopamine autoinhibition	57
Figure 3.4	Hyperpolarization induced inward current (I_h) in VTA neurons	60
Figure 3.5	DAergic neurons have a similar depolarized resting membrane potential as non-DAergic neurons	61
Figure 3.6	DAergic neurons appear to have a slower basal firing rate than non-DAergic neurons	62
Figure 3.7	Afterhyperpolarization profiles of DAergic and non-DAergic neurons	64
Figure 3.8	DAergic neurons have a longer duration action potential than non-DAergic neurons	65
Figure 3.9	Average change in resting membrane potential in response to 1 μ M FPL 64176	67
Figure 3.10	FPL 64176 induces burst firing of VTA DAergic neurons	69
Figure 3.11	FPL 64176 induces burst firing of VTA non-DAergic neurons	70
Figure 3.12	The afterhyperpolarization profile of DAergic and non-DAergic neurons changes during burst firing	71
Figure 3.13	Resting membrane potential of VTA neurons during baseline conditions	73
Figure 3.14	Afterhyperpolarization profile during baseline conditions is related to FPL 64176 induced burst firing	77
Figure 3.15	$Ca_v1.3$ is responsible for modulating burst firing in DAergic and non-DAergic neurons	78

Abstract.....	ii
Acknowledgements.....	iii
List of Abbreviations.....	iv
List of Figures.....	vi

Table of Contents

Chapter 1: Introduction.....	1
1.1 General Introduction.....	1
1.2 The VTA.....	3
1.2.1 Location and composition.....	4
1.2.1.1 Dopamine.....	5
1.2.1.2 GABA.....	10
1.2.2 VTA connectivity.....	11
1.2.3 Central dopamine dysfunction.....	14
1.2.3.1 Addiction.....	14
1.2.3.2 Psychosis/Schizophrenia.....	15
1.3 Firing Patterns.....	17
1.3.1 Synaptic Regulators.....	20
1.3.1.1 DAergic modulation.....	20
1.3.1.2 GABAergic modulation.....	21
1.3.1.3 Glutamatergic modulation.....	23
1.3.1.4 Cholinergic modulation.....	26
1.3.2 Intrinsic channels can modulate firing patterns.....	28
1.3.2.1 Calcium activated potassium channels.....	29

1.3.2.2 KCNQ/M-channel.....	30
1.3.2.3 HCN channel.....	31
1.4 The involvement of calcium	32
1.4.1 Calcium channels	32
1.4.1.1 L-type calcium channels	34
1.5 Rationale and hypotheses for present thesis	35
Chapter 2: Materials and Methods	38
2.1 Animals.....	38
2.1.1 Genotyping.....	39
2.1.1.1 TH-EGFP mouse model.....	39
2.1.1.2 LTCC knock-in mouse model.....	40
2.2 Electrophysiology	41
2.2.1 Slice preparation.....	41
2.2.2 Nystatin-perforated patch clamp recording.....	42
2.2.4 Data analysis	44
2.3 Immunohistochemistry.....	48
2.3.1 Transcardial Perfusion.....	48
2.3.2 Sectioning.....	49
2.3.3 Colocalization of EGFP and TH	49
2.3.5 Image Analysis.....	50
2.3.5.1 Confocal Microscopy.....	50
Chapter 3: Results	51
3.1 Genotyping Results.....	51
3.3 Electrophysiological results.....	55

3.3.1 Basic Electrophysiological Properties.....	55
3.3.1.2 DAergic cells have a larger I_h current.....	58
3.3.2 Other fingerprinting criteria	59
3.3.2.1 Resting membrane potential and basal firing rate of DAergic and non-DAergic neurons are similar	59
3.3.2.2 Spike and afterhyperpolarization profile vary between DAergic and non-DAergic neurons	63
3.3.3 LTCC modulation	66
3.3.3.1 FPL 64176 can induce burst firing in DAergic and non-DAergic neurons ..	66
3.3.3.2 mAHP changes during baseline, bursting, and return to single spike	68
3.3.3.3 Baseline properties and LTCC mediated burst firing	72
3.3.4 LTCC subtype involvement	75
Chapter 4: Discussion	79
4.1 Technical considerations.....	79
4.1.1 Recording method used.....	79
4.1.2 Recording conditions.....	80
4.1.3 Animal model.....	82
4.1.3.1 EGFP driven by the TH promoter efficiently labels DAergic neurons.....	83
4.1.3.2 EGFP vs. other means of identifying cells.....	85
4.2 Basic electrophysiological properties	86
4.2.2 DA autoinhibition is only seen in DAergic cells of the VTA	87
4.2.4 I_h current	88
4.2.5 Afterhyperpolarization profile.....	89
4.2.6 Spike half width	90
4.3 LTCC modulation	92

4.3.1 FPL 64176 can induce burst firing in DAergic and non-DAergic neurons	92
4.3.2 AHP profile and LTCC mediated bursting	95
4.3.3 LTCC subtype involvement	96
4.4 Conclusions.....	98
4.5 Future Directions	100
Reference List.....	102

Chapter 1 - Introduction

1.1 General Introduction

The central nervous system integrates sensory inputs and organizes neuronal output that dictates behavioural responses. A feature unique to the nervous system is that its component neurons do not carry out the work on their own, but rather they form connected networks by way of synapses. A neuron of similar property may be implicated in a different function depending on how it's connected with other neurons in a network through synapses that may use different chemical messengers. As a result, connected networks are often implicated in a particular function. Much like a large company requires a CEO to organize the overall vision of the company, assisted by managers at each department level organizing individual workers in order to successfully function, an organism requires a way to interpret and respond to environmental cues. The CNS is this integration system. Neurons are the “workers” of the CNS. They receive inputs and transform them into outputs. The summed output of a group of neurons (i.e., the department), direct the activity of a system (e.g., motor function). The activity of all systems together directs the behaviour of the organism as a whole, thereby making the brain the “CEO” of the organism.

In this thesis, I will investigate a central dopaminergic (DA) system that is involved in motivation and reward processing. The reward pathway is composed of a group of DA-containing (DAergic) neurons in the ventral tegmental area (VTA) that project to the nucleus accumbens (NAc) and the prefrontal cortex (PFC). In animals such

as rodents and humans, this system drives positive reinforcement, leading to learned motivation (Di Chiara, 1999; Robbins & Everitt, 1996). By interpreting certain stimuli as rewarding (or not rewarding), we learn what actions should be repeated or avoided. Food gathering is one example of an action that requires learned motivation and is essential for survival (Changizi et al., 2002).

Besides the hardwiring of neurons in a network, neurons are also unique in that they are excitable cells that have input and output machinery. This is achieved by the polarized structure of neurons, the basic functional units of the brain, which receive incoming signals from the dendritic tree and generate neuronal output in the form of action potentials in the axon. Both input and output signals are electrical in nature, generated by movement of charged particles across the membrane. There is a fundamental difference between the two in that the input signals in the form of synaptic potentials are graded, whereas the neuronal output in the form of action potentials is all or none. Due to this feature, an individual action potential is limited in the amount of information it can encode; however, a variation in number or pattern of action potentials can tell a very detailed message, much like a limited number of letters can be combined in various patterns to form countless words. The great difficulty in understanding neuronal output is that we do not yet know how information is encoded by a train of action potentials with different temporal patterns. I will concentrate on a particular firing sequence called burst firing in this thesis.

Neuronal excitability depends on network drive by way of synapses and the composition of ion channels on the membrane of an individual neuron that responds to

such a drive. A neuron typically has a great number of ion channels on its membrane. Some of these channels are common to all neurons due to their involvement in generating synaptic and action potentials, for example, the voltage-gated sodium, potassium, and calcium channels. Channel composition of a neuron in some cases is unique to a particular neuronal population so their electrical responses can be used to identify the cell. In this thesis, I will focus particularly on the two isoforms of the L-type calcium channels (LTCCs) that affect the firing of cells in the VTA in a specific manner.

This chapter will provide a brief review of the VTA, a key structure in the reward circuitry, in terms of its cellular composition, connectivity, and more importantly, how firing patterns are regulated in this region. In particular, the chapter will introduce burst firing of DAergic cells in the VTA and how burst firing is brought about in these cells by activation of the LTCCs. This thesis aims to further the understanding of the characteristics of VTA neuronal firing patterns, in the hopes of providing the basis for improved treatment options for disease states connected to VTA neuronal dysregulation.

1.2 The VTA

The VTA is a key structure in the reward circuitry. In rats, selective chemical or electrical ablation of this area results in a loss of reward seeking behaviour while an increase in activity produces an increase in drug seeking behaviour (Di Chiara, 1999). More specifically, a change in activity of the DAergic cells in the VTA results in these behavioural changes. Animals will work to increase the activity of DAergic neurons in the VTA, via electrical or chemical stimulation (Koob, 1992; Koob et al., 1998; White,

2002; Wise, 2002). Conversely, if the DAergic cells of the VTA are destroyed they will no longer display such drug seeking behaviours (White, 2002; Wise, 2002). Similarly, destruction of the other VTA cell population, GABA containing (GABAergic) cells, exaggerates drug seeking behaviours. This cell population exerts a tonic inhibition on DAergic neurons. Subsequently, destruction of this cell population indirectly increases the activity of DAergic neurons. Due to the importance of projections originating in this area in reward processing, the VTA is thought to be the beginning of what is commonly referred to as the “reward pathway”. This section will provide an overview of the VTA with a focus on the importance of DA transmission in reward processing.

1.2.1 Location and composition

The VTA is an area within the ventral midbrain without clear anatomical boundaries and where neurons are scattered diffusely. In general, the level of the caudal tip of the mammillary tract is considered the rostral border and the medial edge of the medial terminal nucleus of the accessory optic tract as the lateral border. It is bordered by other DA-containing midbrain structures, the substantia nigra and retrorubral field. For simplicity, the substantia nigra pars compacta (SNpc) and VTA are typically considered independent structures with distinct physiological functions; however, there is a small overlap between the two structures and their projection targets (Fallon, 1981). With the use of neurochemical markers, for example the vesicular transporter 2 for glutamatergic neurons, tyrosine hydroxylase (TH) for DAergic neurons, and glutamic acid decarboxylase (GAD) for GABAergic neurons, three types of neurons have been found in the VTA. It is estimated that 60-80% are DAergic, 20-40% are GABAergic, and 2-3%

are glutamatergic (Nair-Roberts et al., 2008; Yamaguchi et al., 2007). VTA neurons commonly synthesize and release one or more neuropeptides along with their primary neurotransmitter. For example, many DAergic neurons co-release neuropeptides such as neurotensin or cholecystokinin (Hokfelt et al., 1980), and a small portion of DAergic neurons co-release glutamate (Kaneko et al., 1990).

The two main cell populations of the VTA will be discussed below in terms of their projection targets as well as their inputs.

1.2.1.1 Dopamine

In humans, it is estimated that 70-80% of the brain's DAergic neurons are mainly located in three distinct areas of the midbrain (Taylor & Creese, 2002); the VTA (A10), SNpc (A9) and the retrorubral field (A8) (Nair-Roberts et al., 2008), with the remaining DAergic neurons located primarily in the hypothalamus. Rodents display a similar distribution of midbrain DAergic neurons; however they also have a large population of DAergic neurons in the olfactory bulb (Nair-Roberts et al., 2008; Mclean & Shipley, 1988). Midbrain DAergic neurons are organized in two major systems: the nigrostriatal and mesocorticolimbic systems (Figure 1.1). The nigrostriatal system primarily originates in the SNpc and projects to the dorsal striatum, such as the putamen and caudate nucleus (Moore & Bloom, 1978; Koob, 1996). The mesocorticolimbic system (Figure 1.2) originates in the VTA and mostly projects to the prefrontal cortex and ventral striatum (Fallon & Moore, 1978). The nigrostriatal system plays an important role in movement

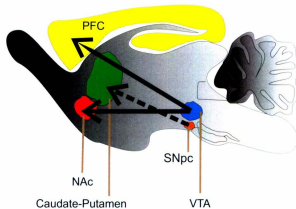


Figure 1.1: **The midbrain DAergic systems.** This simplified diagram shows the major midbrain dopaminergic nuclei and their reciprocal connections. The nigrostriatal system (dashed line) originates in the substantia nigra pars compacta (SNpc) and projects to the putamen and caudate nucleus. The mesocorticolimbic system (solid line) originates in the ventral tegmental area (VTA) and projects to the prefrontal cortex (PFC) and nucleus accumbens (NAc).

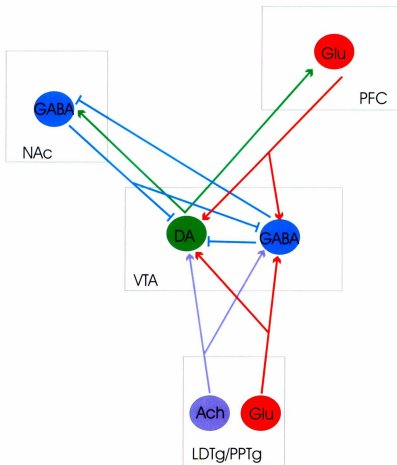


Figure 1.2: **The connectivity of the VTA.** A schematic depicting the major excitatory (arrowheads) and inhibitory (perpendicular line) connections between the VTA and other brain regions. Ach, cholinergic neuron; DA, dopaminergic neuron; GABA, GABAergic neuron; Glu, glutamatergic neuron; LDTg, laterodorsal tegmental area; NAC, nucleus accumbens; PFC, prefrontal cortex; PPTg, pedunculopontine tegmental nucleus.

control—loss of DAergic neurons of the SNpc is the main pathological feature of Parkinson's disease (DeLong, 1990). The mesocorticolimbic system has been most closely connected to motivation and reward (Bjorklund & Dunnett, 2007). Increased DA transmission in this system is associated with addiction and psychosis (Howes & Kapur, 2009; Koob et al., 1998) while ablation of DAergic neurons in this area results in a complete loss of motivation and reward learning (Zhou & Palmiter, 1995).

Prior to the 1970s, DA was thought to be no more than a precursor for norepinephrine. The first support for DA as an independent neurotransmitter came from an assay developed by Arvid Carlsson, enabling the measurement of DA levels in tissue samples, and illustrating that DA was concentrated in specific regions of the brain, some of which did not contain norepinephrine (Carlsson et al., 1958). This was further supported in the early 1970s when Thierry and colleagues demonstrated the synthesis of DA from labelled tyrosine in the cortex (Thierry et al., 1973). Since its discovery as a neurotransmitter, the DA pathways have become of great interest to scientists. Much focus has been on better understanding the regulation of this system as dysregulation in the midbrain DA system has been linked to addiction and psychosis. Zhou and colleagues have illustrated the invaluable role DA plays in the intact organism through the behavioural analysis of dopamine deficient mice (Zhou et al., 1995). Mice missing the enzyme required for dopamine production (and thereby are dopamine deficient) are so unmotivated that they will starve to death before searching out food. If they are hand fed they will eat and survive, but without intervention, they will not take it upon themselves to feed. Interestingly, within minutes of being given a dopamine replacement to restore

dopamine function, their behaviour returns to that of wild type controls (Zhou et al., 1995; Zhou et al., 1990).

DA belongs to a group of neurotransmitters called catecholamines. Their distinctive structural features are a single amine group, a catechol (benzene ring with two adjacent hydroxyl groups) nucleus, and a side chain of ethylamine or one of its derivatives. DA is synthesized from the amino acid tyrosine by the sequential actions of tyrosine hydroxylase (TH; rate limiting step), which generates L-dihydroxyphenylalanine (L-DOPA), and L-aromatic amino acid decarboxylase (AADC). Outside the VTA, some neurons further process DA into norepinephrine by dopamine beta-hydroxylase, which itself can be further processed into epinephrine by phenylethanolamine N-methyltransferase. Once synthesized, DA is actively transported into synaptic vesicles by a vesicular amine transporter (Liu et al., 1994). When released, it acts on the postsynaptic cell by binding to membrane receptors. DA is cleared from synapses by plasma membrane transporters then either degraded by monoamine oxidases or recycled into synaptic vesicles (Amara & Kuhar, 1993).

The diverse physiological actions of DA are mediated by five distinct G protein-coupled receptor subtypes. The receptors have been isolated, characterized, and subdivided into two subfamilies: D1- and D2-like. The D1-like family is comprised of D1 and D5 dopamine receptors and the D2-like subfamily is comprised of D2, D3, and D4 receptors (Missale et al., 1998; Vallone et al., 2000; Andersen et al., 1990). The D1- and D2-receptor have the most widespread and highest levels of expression; both subtypes are expressed in the nigrostriatal and mesocorticolimic pathways. The D1-

receptor is mainly expressed in the caudate putamen, NAc, olfactory tubercle, cerebral cortex, and amygdala, while the D2-receptor is expressed predominantly in the caudate putamen, olfactory tubercle, NAc, SNpc and VTA.

D1-like receptors are positive regulators of cyclic adenosine monophosphate (cAMP) levels through activation of adenylyl cyclase; their stimulation results in the activation of protein kinase A. Protein kinase A in turn phosphorylates cytoplasmic and nuclear proteins, regulates cellular metabolism, including ion channel function, and also desensitizes transmembrane G-protein coupled receptors leading to excitation and neurotransmitter release (Dearry et al., 1990; Dawson et al., 1985; Monsma et al., 1990; Zhou et al., 1990).

The inhibition of adenylyl cyclase activity, however, seems to be a general property of D2-like receptors (Missale et al., 1998). The D2-receptor triggers the inhibition of adenylyl cyclase by coupling to signaling pathways blocked by pertussis toxin (PTX) and K^+ channels (Albert et al., 1990; Neve et al., 1991; Zhou et al., 1990). Therefore, the activation of D2-like receptors can result in an inhibition of the cell.

1.2.1.2 GABA

The other major cell group of the VTA contains the primary inhibitory neurotransmitter in the mammalian CNS, γ -aminobutyric acid (GABA). In the VTA, these cells either communicate locally as inhibitory interneurons or project to cortical and limbic structures (Beart & McDonald, 1980; O'Brien & White, 1987; Churchill et al., 1992). GABAergic interneurons play a significant role in fine tuning the activity of VTA

DAergic neurons. Therefore, understanding characteristics of VTA non-DAergic neurons is vital to further understanding the rewarding and reinforcing properties of drugs of abuse, as well as natural rewarding behaviours ascribed to DAergic neurons.

GABA exerts its effects on target cells by binding to one of two classes of GABA receptors, GABA_A or GABA_B. Activation of GABA_A receptors triggers opening of a chloride-ion selective pore, hyperpolarizing the cell membrane and quickly inhibiting firing. GABA_B receptor activation also leads to cell membrane hyperpolarization but does so by way of G-protein coupled activation of K⁺ channels (Barnard et al., 1998).

1.2.2 VTA connectivity

The DAergic and GABAergic neurons of the VTA communicate with cells in other brain structures via reciprocal projections. Most relevant to reward processing is the information exchange between the VTA and the NAc as well as the VTA and the PFC. This generalized communication loop of VTA neurons with cortical and limbic structures is commonly referred to as the reward pathway.

The connectivity of VTA neurons is, in fact, more widespread than this generalization. The VTA also sends considerable projections to the amygdala, ventral striatum, the ventro-medial part of the head of the caudate-putamen, cingulate cortex, and entorhinal cortex (Bjorklund et al., 2007). As well, VTA neurons receive numerous synaptic inputs from various other brain structures which modulate VTA activity by releasing a variety of neurotransmitters. Major transmitters released in the VTA are GABAergic, glutamatergic, cholinergic, and noradrenergic. Other amino acid terminals

such as glycine or neuropeptides such as neurotensin, substance P, opioids, and orexin also affect cells in the VTA, but are considered minor inputs. The anatomy of the most abundant excitatory and inhibitory inputs will be discussed in this section, with a detailed analysis of their mode of function discussed in later sections.

The major excitatory inputs to VTA cells are glutamatergic projections from the medial PFC and mixed glutamatergic/cholinergic projections from the laterodorsal and pedunculopontine tegmental nuclei (LDTg and PPTg) (Oakman et al., 1995; Woolf & Butcher, 1989; Nair-Roberts et al., 2008; Shi, 2009). Conversely, the major inhibitory inputs to VTA cells come from GABAergic projections or GABAergic interneurons. GABAergic projections originate in either the NAc, which mainly synapse on GABAergic interneurons, or the ventral striatum and pallidum, while GABAergic interneurons synapse mainly on DAergic neurons.

DAergic neurons of the VTA have unmyelinated projections organized in a topographical hierarchy. Those neurons projecting to medial structures are located medially in the VTA while those projecting to lateral structures are located in the lateral portion of the VTA (Ikemoto et al., 1997). DAergic neurons projecting to the medial PFC, basolateral amygdala, NAc medial shell, and NAc core cluster in the medial posterior VTA (paranigral and parabrachial nucleus), with a small population found close to the midline (interfascicular nucleus). Conversely, DAergic neurons projecting to the lateral shell of NAc are almost entirely excluded from the paranigral nucleus and instead are scattered throughout the parabrachial nucleus of the VTA (Lammel et al., 2008). Based on connectivity and morphology, the midbrain DAergic neurons can also be separated

into a dorsal and ventral tier. The dorsal tier cells innervate the ventral striatum, limbic and cortical areas (Bentivoglio & Morelli, 2005). These cells are typically round or fusiform in shape, calbindin-positive, and express low levels of dopamine transporter (DAT) (Bjorklund et al., 2007). The ventral tier is comprised of more densely packed, angular, calbindin-negative cells expressing higher levels of DAT and GIRK2-coupled D2 autoreceptors. Furthermore, studies have identified subpopulations of DAergic neurons with varying properties based upon their projection targets. Lammel et al. have reported an unconventionally fast-firing DAergic population, which selectively project to the prefrontal cortex, core and medial shell of the NAc, and basolateral amygdala (Lammel et al., 2008). As well, they have identified conventionally slow-firing midbrain DAergic neurons that project only to the lateral shell of the NAc. Interestingly, they also provide evidence suggesting mesoprefrontal projecting DAergic neurons do not possess GIRK2-coupled D2 autoreceptors (Lammel et al., 2008). GABAergic neurons are found intermixed with DAergic neurons throughout the VTA, however their distribution is denser in two specific areas (Steffensen et al., 1998). The first is the mid-caudal VTA, dorsal to the lateral parabrachial nucleus where GABAergic cells are similar in size and shape to adjacent TH counterparts. The second is the most caudal VTA, adjacent to the interpeduncular nucleus where GABAergic cells are parvocellular and densely packed into ball-like nuclei.

Through their connections with cortical and limbic structures, projections from the VTA play an important role in the regulation of cognitive functions (Le Moal & Simon, 1991), memory (Lisman & Grace, 2005), emotion (Laviolette, 2007; Pezze & Feldon,

2004), and reward-related behaviors (Koob et al., 1998; Robbins & Everitt, 1999). Specifically, distorted DA output from the VTA has been implicated in diseases such as schizophrenia (Carlsson, 1988; Laviolette, 2007) and drug dependence (Di Chiara & Imperato, 1988; Di Chiara, 1995).

1.2.3 Central dopamine dysfunction

Two disease states associated with dysregulation in the central DA system, addiction and psychosis, are discussed below to highlight the important role the central dopamine system plays in everyday life, as well as the importance of properly regulated DA transmission. While dysregulation can occur at various points in the reward pathway, the common final pathway of both disease states is altered DA transmission.

1.2.3.1 Addiction

Drug addiction is a chronic relapsing disorder characterized by compulsive drug seeking and drug taking behaviours, despite negative consequences. Many drugs of abuse are known to directly or indirectly increase DA transmission in VTA DAergic terminal areas of the NAc and PFC (Di Chiara et al., 1988; Di Chiara, 1995; Imperato et al., 1986), inducing euphoria and reinforcing drug seeking behaviour. Although natural reinforcers also produce an increase in DA release, the effect is not nearly as robust, and unlike addictive drugs, undergoes habituation (Di Chiara, 1999). These differences suggest that drugs of abuse not only 'hijack' a system normally implicated in reward and reinforcing effects of stimuli involved in survival (Robbins et al., 1996), but also the effect is

persistent, adding to the consolidation of responses to drug associated stimuli (Berke & Hyman, 2000) and further promoting the repeated use of addictive substances.

Drugs of abuse such as cocaine and amphetamines primarily enhance DA transmission by blocking DA reuptake and facilitating reverse transport in the terminal (Bradberry & Roth, 1989). Conversely, both nicotine and opiates increase DA transmission in terminal fields through exciting DAergic neurons. Nicotine can directly excite DAergic neurons (Calabresi et al., 1989; Pidoplichko et al., 1997; Picciotto et al., 1998; Pidoplichko et al., 1997) while opiates inhibit the GABAergic inputs to DAergic neurons (Johnson & North, 1992a) leading to disinhibition of the DAergic neurons.

1.2.3.2 Psychosis/Schizophrenia

Schizophrenia is caused by multiple factors involving multiple transmitter systems, however, it is strongly believed that the central DA system plays a significant role in this disease (Carlsson, 1988; Howes et al., 2009). Typical antipsychotic drugs used for the treatment of schizophrenia share an anti-DA activity (Seeman et al., 1976) and drugs which increase DA transmission can exacerbate psychosis. The ability of an antipsychotic drug to suppress positive symptoms of schizophrenia, such as delusions and hallucinations, is strongly correlated with its ability to block D2 receptors. Conversely, atypical antipsychotics, such as clozapine, with a higher affinity to block D1 and D4 receptors over D2 receptors, effectively relieves the negative symptoms of schizophrenia, such as blunted emotion and lack of motivation (Seeman, 1990). This has provided support for the theory that schizophrenia is associated with a differential dysfunction of

the DA systems with hyperactivity in some areas, like the NAc, causing positive symptoms and hypoactivity in other areas like the prefrontal cortex causing negative symptoms (Goto & Grace, 2007). Howes and Kapur (2009) have suggested a new four part hypothesis of schizophrenia in order to broaden the focus of DA deregulation associated with psychosis and emphasize DA dysregulation is associated with psychosis, not all aspects of schizophrenia. Their new hypothesis states: 1) multiple risk factors (e.g., genes, stress and trauma, drug use, and pregnancy or obstetric complications) interact to lead to DA dysregulation—the final common pathway to increase striatal DA and induce psychosis; 2) DA dysregulation is not at the D2 receptor level, but instead at the presynaptic DA control level; 3) DA dysregulation is linked to psychosis rather than schizophrenia; and 4) DA dysregulation is hypothesized to alter the appraisal of stimuli, perhaps through a process of aberrant salience (Howes et al., 2009). The new hypothesis suggests future drug development and research into the cause and development of psychosis should focus on identifying and manipulating the upstream factors that converge on the DA funnel point, instead of relying on current treatment options which act downstream of the critical transmitter abnormality.

In order to understand how dysregulation of the central dopamine system leads to disease states, we must better understand how information is encoded in this system and how this information transmission is modulated. The following section will discuss how information is communicated between brain areas, and how this passage of information is fine tuned in the VTA.

1.3 Firing Patterns

Information is passed from one part of the brain to another in the form of electrical impulses (action potentials; APs). Action potentials have the property of being all-or-none; a cell either fires or it does not. Therefore, a single action potential does not provide much information, but a train of action potentials can provide a very specific message. Information can be encoded in the form of varying frequencies and patterns of action potentials. More specifically, information or messages are exchanged between cells through neurotransmitter molecules. When the AP (depolarization) reaches the axon terminal of a cell it triggers the release of neurotransmitter into the synaptic cleft. Neurotransmitter then acts on the postsynaptic (target) cell, directly or indirectly changing its membrane potential, which changes the excitability state of the cell. The message sent to and from cells is encoded by the change in excitability, through the movement of charged particles in and out of the cell. One neuron may have numerous input terminals, coming from multiple cell types, all sending different messages, as well as intrinsic ion channels whose activity also encode a message. The cell must interpret and integrate all of these messages in order to create an output to the cells it directs. It must determine whether or not to fire APs (depolarization or hyperpolarization), as well as the frequency and pattern this should occur in.

Neurons of the CNS can fire action potentials in two patterns: single spike (tonic), or bursts (Figure 1.3). Within each pattern, there can be a large variation. Single spike firing can have a regular (pacemaker) or irregular pattern, leading to different patterns of neurotransmitter release. Burst firing is characterized as a series of action potentials fired

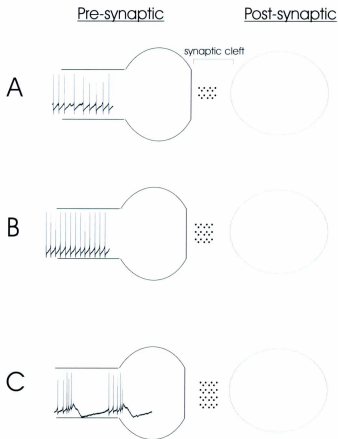


Figure 1.3: **Firing patterns of midbrain neurons.** A) During slow single spike firing small amounts of DA are released into the cleft. B) During higher frequency single spike firing more DA is released. C) Burst firing causes the highest amount of DA to be released into the cleft where it saturates reuptake transporters and DA autoreceptors. DA released from burst firing stays in the synaptic cleft longer and therefore causes stronger postsynaptic effects.

in close succession (an intraburst frequency higher than previous single spike frequency) followed by a strong afterhyperpolarization (AHP) tail. The number of APs within a burst can vary greatly, as can the interval between bursting cycles. Burst firing results in more neurotransmitter being released into the synapse in a short period of time, leading to saturation of reuptake transporters and autoreceptors. This allows more neurotransmitter to remain in the cleft (and for longer), increasing the interaction with postsynaptic receptors, and thereby causing burst firing to be a more efficient mode of transmission than single spike firing. Because the pattern of AP firing carries so much information, understanding the mechanisms behind firing pattern regulation is invaluable. As previously discussed, dysregulation of the DA pathway originating in the VTA has been implicated as the underlying cause of various disease states. Understanding DAergic and GABAergic neuron firing regulation can help better understand the dysregulation of DA transmission, and thereby potentially lead to better treatment options.

Using behaviour studies, various groups have illustrated the importance of variation in firing patterns. Freeman and Bunney have shown that burst firing in behaving rats is associated with the presentation of a novel stimulus (Freeman & Bunney, 1987) while Schultz and colleagues have shown this in greater detail in monkeys (Schultz et al., 1997; Schultz, 1998). Schultz and colleagues demonstrated that midbrain DAergic neurons are activated by a primary reward, especially if it is unexpected (Schultz et al., 1997; Schultz, 1998). If the reward is coupled with a conditioned stimuli, DAergic neurons switch from regular single spike firing to burst firing or increase their rate of firing from the moment of the conditioned stimulus to the instant when the reward

appears. If the conditioned stimulus is not followed by the expected reward the DAergic neurons decrease their firing. The DAergic neuron can thus detect a discrepancy from the expected reward so that a positive signal is delivered to the brain if the reward is better than expected, no change if the reward is as expected, and negative signal if less than expected. The firing activities of the DAergic neurons signal the occurrence of novel and rewarding stimuli, and changes in firing activity affects target areas.

1.3.1 Synaptic Regulators

There are a variety of neurotransmitters in the brain, each having very specific modes of action. This section will primarily focus on firing pattern modulation via DAergic, GABAergic, glutamatergic, and cholinergic neurotransmitters before exploring how intrinsic channel expression also influences firing patterns of VTA neurons.

1.3.1.1 DAergic modulation

There are various DA receptor subtypes expressed in the CNS. DA autoreceptors are D₂/D₃ receptors (D-2 like subfamily) and are located in the axon and somatodendritic region of DAergic neurons (Clark & Chiodo, 1988; Mercuri et al., 1992a). They are activated by synaptically and somatodendritically released DA (Beart et al., 1979; Cheramy et al., 1981; Kalivas & Duffy, 1991) and reduce DAergic neuron activity by activating GIRK channels, presumably via G protein $\beta\gamma$ subunits that are liberated by receptor activation of G_{i/o} proteins. This produces a hyperpolarization of the cell body to inhibit firing, thus causing the terminals to cease releasing DA (Mercuri et al., 1992a; Innis & Aghajanian, 1987; Williams & Lacey, 1988; Morikawa et al., 2003; Lacey et al.,

1987). Moreover, the sensitivity of autoreceptors affects how the cell fires; fast firing DA neurons have been shown to have sub-sensitive autoreceptors, while slow-firing neurons exhibit greater sensitivity of these receptors (Marinelli & White, 2000; White & Wang, 1984) as revealed by the dose dependent neuronal inhibition following local administration of D₂/D₃ receptor agonists into the VTA (Akaoka et al., 1992; Gariano et al., 1989; Pucak & Grace, 1994). This effect is independent of differences in neuronal inputs because slow-firing cells are more sensitive to autoreceptor-mediated inhibition even when they are driven to a faster firing rate by local application of glutamate (White et al., 1984). Overall, these findings suggest that the functional state of somatodendritic DA autoreceptors mediates the activity of DAergic neurons.

1.3.1.2 GABAergic modulation

The major GABAergic inputs to the VTA originate from the NAc (onto GABAergic cells), and the ventral striatum and pallidum (onto DAergic neurons). As well, there is a strong GABAergic input from midbrain interneurons. The presence of GABAergic interneurons within the VTA explains many biphasic effects produced by stimulation of brain structures projecting to the midbrain or by systemic pharmacological treatments. Stimulation of afferents onto DAergic neurons can have an initial response that is immediately followed by an opposite response. This biphasic response is seen because afferents can form synapses onto both DAergic and GABAergic neurons in the VTA. Synapses onto DAergic cells produce direct inhibition while synapses onto GABAergic interneurons may produce indirect excitation of DAergic cells by inhibiting local GABAergic interneurons. Synapses onto GABAergic interneurons will directly

change the activity of the GABAergic neurons, subsequently modifying the activity of DAergic neurons. Therefore, synapses onto GABAergic interneurons can indirectly result in an opposite modulation of DAergic neurons. For this reason, systemic administration of GABAergic drugs can have a 'paradoxical' effect on DAergic neurons (Waszczak & Walters, 1980; Grace & Bunney, 1979).

GABA acts on a post-synaptic cell by binding to one of two classes of GABA receptors, GABA_A or GABA_B. Binding of GABA molecules to the binding sites of the extracellular part of GABA_A receptors triggers the opening of a chloride-ion selective pore, resulting in cell hyperpolarization (Johnson et al., 1992a). Local application of the GABA_A receptor agonist muscimol induces a clear inhibition of DAergic neurons on a fast time scale (Erhardt & Engberg, 2000). Conversely, the selective GABA_A receptor antagonists bicuculline, gazabine, and picrotoxin enhance both firing rate and bursting activity of DAergic neurons.

In contrast to GABA_A receptors, GABA_B receptors mediate inhibition on a slower time course via G-protein coupled activation of K⁺ channels. Activation of these channels allows K⁺ ions to flow out of the cell, resulting in hyperpolarization of the cell membrane. Microinjection of the GABA_B receptor agonist baclofen into the VTA reduces DAergic neuron firing and converts burst firing to single-spike firing, (Erhardt et al., 2002; Tsuji et al., 1996). Conversely, the application of GABA_B receptor antagonists increases DAergic neuron firing rate and bursting frequency (Chen et al., 2005; Erhardt et al., 1998; Engberg et al., 1993). Activating or blocking GABA_B receptors on presynaptic glutamate terminals suppresses or attenuates, respectively, excitatory transmission onto

GABAergic interneurons, altering the tonic inhibition exerted by these neurons on DAergic cells (Wu et al., 1999).

GABA afferents from the striatal complex also play an important role in certain conditions, such as after the administration of psychostimulant drugs (Einhorn et al., 1988); (Pitts et al., 1993). After the injection of kainic acid, a glutamate agonist, into the dorsal striatum, there is a transient decrease in the activity of DAergic cells due to depolarization inactivation (Braszko et al., 1981). The injection of kynurenic acid, a glutamate receptor antagonist, into the NAc produces a transient decrease in firing rate and burst firing of VTA DAergic neurons (Floresco et al., 2001). Notably, hemitransection of this striatal-VTA pathway fails to modify basal impulse activity on VTA DAergic neurons (Einhorn et al., 1988; Pitts et al., 1993; Pucak et al., 1994).

1.3.1.3 Glutamatergic modulation

As discussed in section 1.2.2, the VTA receives direct and indirect glutamatergic inputs from the PFC, LDTg, and PPTg (Carr & Sesack, 2000). An increase in glutamatergic drive enhances neuronal activity and induces burst firing of DAergic cells *in vitro* (Meltzer et al., 1997). Electrical stimulation of the medial PFC enhances DAergic neuron activity and produces burst firing (Gariano & Groves, 1988; Tong et al., 1996). Inactivation of this projection by cooling the cortex or administration of glutamate receptor antagonists reduces the firing rates and bursting, replacing it with pacemaker-like activity (Tong et al., 1996). Activation of the PPTg also enhances VTA firing activity and induces burst firing of DAergic cells (Lokwan et al., 1999). Furthermore,

pressure-injected glutamate in the VTA increases the firing rate of DAergic cells, thereby increasing the extracellular DA concentration in projecting areas such as the NAc (Suaud-Chagny et al., 1992).

Glutamate acts via three general groups of receptors that are expressed on VTA neurons: AMPA, NMDA, and metabotropic (Catania et al., 1994). Both AMPA and NMDA receptors are ion channels that are opened by glutamate binding and allow sodium and calcium to move into the cell, whereas metabotropic glutamate receptors (mGluRs) bind glutamate and modulate ion activity via second messenger systems.

AMPA and NMDA receptors mediate the majority of excitatory input to midbrain DAergic neurons. *In vivo* studies have shown that application of both NMDA and AMPA receptor agonists increase firing of spontaneously active DAergic neurons of the VTA; however, bursting activity in the VTA appears to be AMPA receptor independent (Christoffersen & Meltzer, 1995; Zhang et al., 1994). Studies in the tissue slice show the excitatory role of these receptors; application of either AMPA or NMDA evokes an inward current and increases neuronal firing in a dose dependent manner (Mercuri et al., 1992b; Wang & French, 1993a; Wang & French, 1993b). At a low dose ($\leq 30\mu\text{M}$), glutamate's effect on firing rate and membrane potential are mostly NMDA receptor mediated, as application of the non-competitive NMDA blocker phencyclidine and the selective competitive NMDA receptor antagonist CGS 19755 completely abolish these effects (Wang et al., 1993a). NMDA receptor activation has also been shown to induce burst firing, particularly in the presence of hyperpolarizing currents or when calcium-activated potassium currents are blocked by apamin (Johnson & Seutin, 1997; Seutin et

al., 1993; Johnson & Wu, 2004). The mechanism underlying NMDA induced burst firing can involve different ion species. For example, it has been suggested that Na^+ influx via NMDA-gated channels and the subsequent removal of Na^+ by the ouabain-sensitive electrogenic Na^+ pump comprises the full cycle of bursting (Johnson et al., 1992c). These findings underline the important excitatory role of AMPA and NMDA glutamate receptor activation in VTA neuron regulation.

Activation of mGluRs can be either excitatory or inhibitory, depending on how the receptors are activated. Fast activation of post synaptic group 1 mGluRs via synaptically released glutamate results in the mobilizing of calcium stores, which activates inhibitory calcium-dependent potassium channels, mediating slow inhibition (Fiorillo & Williams, 1998). With prolonged activation this inhibitory response desensitizes. Continuous activation of group 1 mGluRs can lead to an increase in DAergic cell activity due to a slowly-developing sodium-dependent excitation (Mercuri et al., 1993; Fiorillo et al., 1998; Zheng & Johnson, 2002). Activation of mGluRs can also modify DAergic neuron activity indirectly by acting on presynaptic glutamatergic terminals, modifying glutamate release. Dependent upon the resulting activation of the phospholipase C pathway, presynaptic mGluR activation can have excitatory or inhibitory effects, producing enhanced or decreased, respectively, NMDA-mediated excitation in postsynaptic cells (Herrero et al., 1992). Similarly, bath application of high doses of glutamate has been shown to enhance DAergic neuron firing, as well as temporarily inhibit firing through activation of NMDA and AMPA receptors or mGluRs (Kim et al., 2004). The group 1 mGluRs have also been shown to play a role in the regulation of the

firing pattern of midbrain DAergic neurons, especially in the SNpc (Meltzer et al., 1997). In the presence of SK channel blockers, the group 1 mGluR agonist (s)-3,5-dihydroxyphenylglycine can transform SNpc DAergic cells from single spike firing to bursting (Prisco et al., 2002). Furthermore, the mGluR antagonist s-methyl-4-carboxyphenylglycine [(s)-MCPG] blocks the post-burst hyperpolarization in DAergic neurons where bursting had been induced by repetitive extracellular stimulation or ionophoretic application of aspartate (Morikawa et al., 2003).

Together, these findings indicate that bursting may be ascribed, at least in part, to a complex combination of glutamate receptors. Activation of these receptors can exert both excitatory and inhibitory roles, either directly or indirectly, by modifying glutamate release or activity of other channels.

1.3.1.4 Cholinergic modulation

Cholinergic input, mainly from the LDTg and PPTg, has been shown to play a vital role in regulating the firing activities of VTA neurons. Electrical or chemical stimulation of the LDTg or PPTg has been shown to increase firing activity of VTA DAergic neurons, as well as result in a prolonged increase of DA release in the NAc (Floresco et al., 2003; Forster et al., 2002). Similarly, inactivation of the LDTg produces a pronounced decrease in burst firing of VTA DAergic neurons that is not rescued by PPTg stimulation (Lodge & Grace, 2006).

The effects of cholinergic input are due to two general groups of receptors: nicotinic and muscarinic acetylcholine receptors (AChR). Neurons in the VTA express

somatic and dendritic nicotinic (Clarke & Pert, 1985; Clarke et al., 1985; Sorenson et al., 1998) and muscarinic (Nastuk & Graybiel, 1991) AChRs.

Nicotinic receptors are crucial in the initial fast response to ACh and mediate addiction (Balfour et al., 2000). Acute systemic administration of nicotine increases intracranial self-stimulation rates (Druhan et al., 1989) and locomotor activity in rats (Picciotto et al., 1998), while infusion of a nicotinic antagonist in the VTA results in a significant reduction in nicotine self-administration (Corrigall et al., 1994) and nicotine induced locomotor activity (Louis & Clarke, 1998). As well, systemically administered nicotine increases extracellular DA in the NAc, due to increased firing rate and burst firing activity of VTA DAergic neurons. This increase in NAc DA can be blocked by infusion of the nicotinic receptor antagonist mecamylamine into the VTA, but not into the NAc (Grenhoff et al., 1986; Nisell et al., 1994). Infusion of nicotine directly into the VTA produces an increase in the firing rate of spontaneously firing DAergic neurons or a depolarization of membrane potential generating action potentials in quiescent neurons, and is followed by a rapid desensitization (Calabresi et al., 1989; Pidoplichko et al., 1997; Sorenson et al., 1998). Furthermore, nicotinic receptors are shown to mediate presynaptic effects by enhancing glutamate release. Nicotine has been shown to increase evoked and spontaneous excitatory synaptic currents in VTA DAergic neurons (Dani & De Biasi, 2001; Mansvelter & McGehee, 2000).

Muscarinic receptors are responsible for the prolonged response to ACh seen in DAergic cells (Lacey et al., 1990) and are implicated in reward processing. Infusion of atropine, a nonselective muscarinic receptor antagonist, into the rat VTA decreases self-

stimulation and reduces food intake (Rada et al., 2000). *In vivo*, activation of postsynaptic M₁-like muscarinic receptors evokes a slow depolarization with an increase in firing rate and burst firing (Lacey et al., 1990; Zhang et al., 2005). Besides M₁ and M₅ receptor subtype mediated postsynaptic excitation, muscarinic agonists can also potentially increase DAergic neuron firing rates indirectly by reducing GABAergic transmission via postsynaptic M₃ receptors (Grillner et al., 1999). Furthermore, muscarinic agonists are able to decrease afterhyperpolarizations, allowing DAergic cells to fire at a higher frequency and possibly burst fire (Scroggs et al., 2001).

Muscarinic receptors are shown to be coupled to G_q or G_{i/o} activating phospholipase C, leading to the hydrolysis of polyphosphoinositol (PPI) or inhibiting adenylyl cyclase so as to affect different ion channels (Caulfield, 1993; Hulme et al., 1990). It is believed that AChR activation leads to an increase of intracellular calcium concentration mediated through NMDARs (Kitai et al., 1999), LTCCs (Zhang et al., 2005) and the mobilization of internal calcium stores, supporting the idea that a changes in firing patterns following AChR activation is a calcium-dependent mechanism.

1.3.2 Intrinsic channels can modulate firing patterns

Section 1.3.1 discussed presynaptic receptors and channels that contribute to changing a cell's excitability in response to neurotransmitter signalling. There are also channels distributed along the cell body and axons (somatodendritic area) that contribute to fine tuning cell excitability. There are significant differences between the spontaneous activity of midbrain DAergic neurons *in vitro* and *in vivo* suggesting that afferent input

plays a role in modulating the activity, particularly the firing pattern of these neurons (Grace & Bunney, 1984). DAergic neurons *in vivo* will spontaneously burst fire (even in anesthetised rats, not responding to novel stimuli), a behaviour rarely seen *in vitro* (where all afferent inputs are severed). However, *in vitro*, DAergic neurons with single spike baseline firing can burst fire in response to various manipulations of intrinsically expressed channels (Blythe et al., 2007; Shepard & Bunney, 1988; Blythe et al., 2007; Shepard et al., 1988; Liu & Chen, 2008; Zhang et al., 2005). The following section will provide a brief overview of a selection of intrinsically expressed channels most relevant to cells in the VTA.

1.3.2.1 Calcium activated potassium channels

Calcium activated potassium channels selectively conduct K^+ over other monovalent ions and their activity is enhanced by increased intracellular calcium. Based on their K^+ permeability, 3 types of calcium activated potassium channels have been recognized: those of big (BK), intermediate (IK), and small (SK) conductance (Sah, 1996; Brodie et al., 2007). The CNS contains BK and SK channels, with research in the VTA mostly focusing on SK channels. SK channels contribute to the shaping the AHP of spontaneous and evoked APs in these neurons (Bond et al., 2004; Waroux et al., 2005). That is, when internal calcium concentration increases (after an AP for example) SK channels open, resulting in K^+ leaving the cell (hyperpolarization).

Application of very low doses of apamin, the SK blocker, *in vitro* has been shown to interrupt the pacemaker activity of dopamine neurons in the SNpc, and facilitate

bursting activity produced by application of excitatory amino acids (Seutin et al., 1993). The transition between slow irregular firing and burst firing is also controlled by fluctuations in membrane potential, which are also modulated by SK channels.

1.3.2.2 KCNQ/M-channel

KCNQ genes encode for five subunits, KCNQ 1-5, which form homo- and heterodimeric voltage gated potassium channels (Nakajo & Kubo, 2005). KCNQ2 and KCNQ3 subunits are widely expressed in peripheral and central neurons (Smith et al., 2001; Weber et al., 2006) where they give rise to a muscarinic-sensitive, non-inactivating K^+ current (M-current), active near action potential threshold. Given that M-channels function at depolarized membrane potentials, they play an important role in regulating firing patterns by acting as a brake on repetitive action potential discharges (Lacey et al., 1990; Cox et al., 1998). Studies in hippocampal neurons have shown M-channels are activated during spike afterdepolarization, limiting the duration of depolarization and therefore preventing the generation of burst firing (Yue & Yaari, 2004). This M-channel control of firing patterns has also been seen in VTA DAergic cells. Both *in vivo* and *in vitro* studies have shown a reduction in VTA DAergic neuron excitability in the presence of the M-channel opener retigabine (Hansen et al., 2006) and an increase in firing rate in the presence of the M-channel blocker XE-991 (Koyama & Appel, 2006). Additionally, in dissociated DAergic neurons, blocking M-current shortens the interspike interval and consequently increases firing frequency (Koyama et al., 2006). Considering AHPs play a fundamental role in shaping firing patterns (Alger & Williamson, 1988; Overton & Clark, 1997), it would be expected that M-channels, through their AHP modulation, participate

in generating burst firing in VTA DAergic cells. This can be seen *in vitro*, where some single spiking VTA DAergic neurons begin to burst fire when muscarinic agonists inactivate M-currents (Zhang et al., 2005).

1.3.2.3 HCN channel

Hyperpolarization-activated and cyclic-nucleotide-gated (HCN) channels, as the name suggests, are activated at hyperpolarized membrane potentials and are regulated by the binding of cAMP. When active, they direct an inward current (depolarization). Typically the value of activation is between -70 and -90mV (Wahl-Schott & Biel, 2009). Unlike most other voltage-gated currents, the current flowing through HCN channels (termed I_h) does not inactivate in a voltage-dependent fashion.

HCN are non-selective ion channels that conduct Na^+ and K^+ with permeability ratios of about 1:4. Despite this preference for K^+ conductance, HCN channels carry an inward Na^+ current under normal physiological conditions. HCN channels also seem to display a small permeability for calcium. Because these channels open at hyperpolarized potentials, Na^+ will enter the cell when HCN channels are open resulting in a depolarization. This current contributes to several neuronal processes, including determination of resting membrane potential, dendritic integration, and synaptic transmission. Following an action potential, there is an “overshooting” of the resting membrane potential, or afterhyperpolarization. HCN channels are one component of “fixing” the hyperpolarization and restoring the membrane to its resting membrane potential. Due to their slow kinetics, HCN channels contribute greatly to the slow

component of AHPs. Large I_h currents have been seen in VTA DAergic neurons, and contribute to the long inter-burst intervals seen between bursting cycles.

1.4 The involvement of calcium

Neuronal firing patterns are strongly regulated by changes in intracellular calcium concentrations. In midbrain DAergic neurons, intracellular injection of calcium in high concentrations *in vivo* increases burst firing, whereas introduction of the calcium chelator EGTA reduces the depolarization that initiates bursting and thus also greatly reduces bursting (Grace et al., 1984). It is clear that calcium regulates the firing pattern of midbrain DAergic neurons and work from our lab has implicated LTCCs as the route of calcium entry to mediate this action (Liu et al., 2008; Liu et al., 2007; Zhang et al., 2005). The following section will discuss general properties of voltage gated calcium channels (VGCCs), as well as work which supports their involvement in firing pattern modulation of VTA neurons.

1.4.1 Calcium channels

Intracellular calcium concentration plays a pivotal role in a multitude of cellular processes including, but not limited to, gene expression, muscle contraction, synaptic plasticity, and neurotransmitter release. Among the many channels and pumps involved in controlling intracellular calcium levels, VGCCs play a key role. *In vivo* these channels open and close according to changes in membrane potential, hence the name “voltage gated”. When open, VGCCs allow calcium to move into the cell.

VGCCs have been classified based upon electrophysiological and pharmacological properties, as well as amino acid composition, as either high voltage activated (HVA) or low voltage activated (LVA). HVA channels include L-, N-, P-/Q-, and R-types while LVA channels are T-type. In general, HVA channels open at membrane potentials higher than average resting membrane potentials (i.e., a depolarization) while LVA channels open at membrane potentials more negative than average resting membrane potentials (i.e., a hyperpolarization). With respect to candidates that may influence firing pattern modulation, the HVA channels would be the main contender. In order to convert single spike firing to burst firing, the depolarization needs to be extended, allowing multiple APs to fire within a single depolarization.

VGCCs are heteromeric complexes of five proteins: a) the pore-forming α_1 subunit which contains the binding sites for calcium channel modulators, the voltage sensor, and the selectivity filter; b) a transmembrane, disulfide-linked dimer of α_2 and δ subunit; c) an intracellular β subunit; and d) the transmembrane γ subunit (Walker & De Waard, 1998). Molecular biology studies have identified ten different genes each coding for a different α_1 subunit. They are divided into three subfamilies, Ca_v1, Ca_v2, and Ca_v3, based upon their sequence similarities. The Ca_v1 isoforms correspond to L-type channels, Ca_v2 isoforms represent N-, P-/Q-, R-channels, and the Ca_v3 isoforms form the T-type channels.

All VGCC types are expressed in the CNS; however each class has a distinct distribution pattern, leading to a specific physiological role. For example, LTCCs are found mostly on the cell body while N-type are highly concentrated in presynaptic

terminals and dendrites (Takada et al., 2001; Westenbroek et al., 1992). By examining the distribution patterns and properties of each HVA subtype, the most likely candidate for modulation of firing patterns in VTA neurons is the LTCC. These channels are responsible for approximately one third of the total calcium currents in DAergic cells (Cardozo & Bean, 1995; Durante et al., 2004; Takada et al., 2001) and contribute preferentially to whole-cell calcium currents evoked by small depolarizations (Durante et al., 2004; Xu & Lipscombe, 2001). *In vitro* studies show that LTCC agonists produce membrane depolarization and subsequently increase firing rates, while antagonists reduce membrane depolarization and decrease firing rates (Cardozo et al., 1995; Chan et al., 2007; Mercuri et al., 1994; Zhang et al., 2005). Burst firing and the underlying depolarizing membrane potential oscillation induced by cholinergic activation in slice preparations can be prevented by the LTCC antagonist nifedipine (Zhang et al., 2005).

1.4.1.1 L-type calcium channels

There are four LTCC subtypes, ($\text{Ca}_v1.1 - 1.4$; α_{1S} , α_{1C} , α_{1D} , α_{1F}), which are modulated by three classes of drugs: dihydropyridines (DHP), phenylalkylamines (PAA), and benzothiazepines (BTZ), all of which bind to sites in the α_1 subunit. $\text{Ca}_v1.2$ and 1.3 isoforms are found in neuronal cells, as well as cardiac smooth muscle and pacemaking cells. They have been given the L-type distinction based upon their “long-lasting” currents; unlike other voltage gated channels, LTCCs have calcium-dependent inactivation with little voltage-dependent inactivation (Lipscombe et al., 2004). DAergic and GABAergic neurons within the VTA express the $\text{Ca}_v1.2$ and $\text{Ca}_v1.3$ subtypes (Hell et al., 1993). Previous work from our lab demonstrated calcium influx through LTCCs is

required for bursting to occur in VTA DAergic cells (Zhang et al., 2005). The sequences of both LTCC subtypes expressed in the VTA differ only in a small segment between the II and III domain of the α_1 subunit. Due to this high sequence similarity, they cannot be selectively targeted by pharmacological agents, making it difficult to evaluate which subtype is responsible for modulating firing patterns. Using a mouse model with a point mutation in the $\text{Ca}_v1.2$ DHP binding site and EGFP labelled DAergic neurons, we concluded $\text{Ca}_v1.3$, which operates at close to resting membrane potentials, regulates burst firing in DAergic and GABAergic neurons (unpublished).

1.5 Rationale and hypotheses for present thesis

Previous studies have identified the importance of calcium messaging in modulating firing patterns in DAergic VTA neurons. Work from our lab showed, *in vitro*, direct LTCC activation converts spontaneous single spike firing to burst firing in putative DAergic neurons (Zhang et al., 2005). Further investigation suggested LTCC activation leads to increased PKC, and as a result PKM, activity which is required for bursting to occur (Liu et al., 2008; Liu et al., 2007).

Recently, several groups have provided evidence suggesting the widely accepted electrophysiological fingerprinting criteria used in these studies results in selecting a subpopulation of DAergic neurons, with the potential of including some GABAergic neurons as well (Margolis et al., 2006; Lammel et al., 2008). Since our previous work used these identification criteria, we wanted to investigate the validity and accuracy of electrophysiological fingerprinting criteria, as well as investigate the effects of LTCC

modulation on GABAergic neurons of the VTA. As previously discussed, GABAergic neurons fine tune the activity of DAergic neurons and project to similar target areas as DAergic neurons, however the functional outcome of DAergic and GABAergic innervations are very different. It is important to understand how the firing pattern and activity of both cell populations of the VTA is modulated in order to provide better insight into disease states associated with altered DA transmission.

This thesis will first look at the electrophysiological characteristics of DAergic and GABAergic VTA neurons, where I hypothesize that there is a difference in intrinsic electrophysiological properties between populations. In these experiments I asked whether or not basic electrophysiological properties can provide an accurate means of identifying the neurotransmitter content of VTA neurons.

Next I looked at the response of DAergic and GABAergic VTA neurons to LTCC modulation. Since LTCC mediated bursting had already been seen in DAergic neurons (Zhang et al., 2005; Liu et al., 2008), but was not previously investigated in GABAergic neurons, I hypothesized that LTCC activation would induce burst firing in DAergic but not GABAergic neurons. Given the opposite functional outcome of DAergic and GABAergic excitation, I expected LTCC activation would lead to inhibition of GABAergic neurons.

Building upon the results of the previous experiment—LTCC activation induces burst firing in DAergic and GABAergic VTA neurons—my final set of experiments sought to answer whether different LTCC subtypes mediate burst firing in DAergic and

GABAergic neurons. In order to test the hypothesis that a different LTCC subtype mediates burst firing in each cell population, a Ca_v1.2 transgenic mouse strain with EGFP labelled DAergic neurons was used.

Chapter 2 - Materials and Methods

Protocols involving animal housing and tissue harvesting were in accordance with guidelines set by the Institutional Animal Care Committee at Memorial University. Care was taken to use the minimal number of animals required to achieve statistical significance.

2.1 Animals

All mice were housed in a temperature controlled (22°C) facility under a 12 hour light/12 hour dark cycle (8 am – 8 pm light, 8 pm – 8 am dark) with food and water available *ad libitum*. Mice were weaned when they were 21 days old and housed with same sex siblings to a maximum of four mice per cage.

Transgenic mice expressing enhanced green fluorescent protein (EGFP) driven by the tyrosine hydroxylase (TH) promoter (TH-EGFP^{+/+} with C57BL/6J background; Matsushita et al., 2002) were bred with transgenic mice carrying a mutant DHP site in the α -1 subunit of Ca_v1.2 L-type calcium channels (Ca_v1.2 DHP^{-/-} with C57BL/6 background; Striessnig et al., 2006) to yield the mice used for this study (EGFP^{+/+}Ca_v1.2 DHP^{+/+} and EGFP^{+/+}Ca_v1.2 DHP^{-/-}). Breeder pairs of one male per two females were used to maintain the colony.

EGFP expression driven by the TH promoter allowed dopaminergic (DAergic) cells to give off green fluorescence under 488 nm light. The fluorescent protein exists in all catecholamine neurons; within the VTA DAergic neurons are the only cells expressing a

catecholamine. A point mutation of the DHP site dramatically decreases the sensitivity of Ca_v1.2 L-type calcium channels to DHP modulators. By using both DHP and non-DHP mediated LTCC agonists, Ca_v1.2 and Ca_v1.3 could be selectively modulated.

2.1.1 Genotyping

During weaning mice were ear tagged and a tail segment of about 1 cm was cut for genotyping. Bleeding was generally minor and could easily be stopped with silver nitrate. Mouse tail segments were placed in 1.5 mL microcentrifuge tubes which were filled with 600 μ L lysis buffer/proteinase K solution (composition: 99 mM Tris-HCl pH 8.0, 4.95 mM EDTA pH 8.0, 0.198% SDS, 0.2 M NaCl, 0.02% proteinase K). They were shaken at 180 rpm overnight at 50°C then centrifuged at 21 000 xg, 4°C, for 30 min. The aqueous phase was decanted into a new microcentrifuge tube, 1 mL 100% ethanol was added, and the tube was inverted multiple times and placed in a -20°C freezer for 2 hours to precipitate DNA. The samples were again centrifuged at 21 000 xg, 4°C, for 30 min and the supernatant was gently removed. The remaining DNA pellet was air dried before 75-100 μ L TE pH 8.0 (10 mM Tris-HCl and 1 mM EDTA) was added and the pellet dissolved at 70°C for 3-4 hr. Once the DNA pellet was dissolved the samples were kept at 4°C until analyzed by PCR. All primers used for genotyping were purchased from Integrated DNA Technologies (Iowa, USA).

2.1.1.1 TH-EGFP mouse model

PCR mix was prepared as follows: 1 x Taq Buffer (Invitrogen, Ontario, Canada), 0.2 μ M dNTP's (Invitrogen, Ontario, Canada), 0.5 μ M GFPnl-up primer (5'-

GACGTAAACGGCCACAAGTTC-3', Integrated DNA Technologies, Iowa, USA), 0.5 μ M GFPnl-Iw (5'-CTTCTCGTTGGGGTCTTTGCT-3', Integrated DNA Technologies, Iowa, USA), 0.5 μ L Platinum Taq polymerase (Invitrogen, Ontario, Canada), 3 μ L DNA, and water to a final volume of 30 μ L. To amplify EGFP DNA, PCR samples were run as follows: first at 94°C for 60sec, followed by 32 cycles of [60 sec at 94°C, 60 sec at 55°C, and 40 sec at 72°C], then 72°C for 60 sec, and finally held at 4°C.

DNA samples from the PCR reaction were prepared by adding 1x DNA loading buffer to each reaction tube before 20 μ L was loaded into a 2.5% agarose gel containing ethidium bromide and electrophoresed at 160 mV for 20 min. DNA bands in the gel were photographed under UV light. As homozygous expression of EGFP was lethal by postnatal day 21 all homozygous EGFP expressing mice died before genotyping began. Therefore, any mice with a DNA band at 582 bp were considered heterozygous EGFP (TH-EGFP^{+/+}) while mice with no visible DNA band were considered wild type (TH-EGFP^{-/-}).

2.1.1.2 LTCC knock-in mouse model

The PCR mix was prepared as follows: 1 x Taq Buffer (Invitrogen, Ontario, Canada), 0.2 μ M dNTP's (Invitrogen, Ontario, Canada), 0.2 μ M Loxup2 primer (5'-TCCTGCACTTAGGTAAGCAAAGGC-3', Integrated DNA Technologies, Iowa, USA), 0.2 μ M Screen1 primer (5'-GAACATGAACTGCAGCAGAGTGGT-3' Integrated DNA Technologies, Iowa, USA), 0.2 μ M alewt primer (5'-GAACATGAACTGCAGCAGAGTGTA-3', Integrated DNA Technologies, Iowa, USA),

0.5 μ L Platinum Taq polymerase (Invitrogen, Ontario, Canada), 5 μ L DNA, and water to a final volume of 30 μ L. To amplify normal and mutated Ca_v1.2 DNA, PCR samples were run as follows: first at 94°C for 5 min, followed by 30 cycles of [30 sec at 94°C, 30 sec at 64°C and 30 sec at 72°C] and finally held at 4°C.

DNA samples from the PCR reaction were prepared by adding 3 μ L 10x DNA loading buffer (0.417% bromophenol blue, 0.417% xylene cyanol, and 25% Ficoll type 400 in water) to each reaction tube. 20 μ L was loaded into a 2.5% agarose gel containing TAE buffer and electrophoresed at 160 mV for 20 min. DNA bands in the gel were visualized with ethidium bromide staining and photographed under UV light. Wild type mice (Ca_v1.2 DHP^{+/+}) had a DNA band at 390 bp corresponding to the normal Ca_v1.2 channel; mice homozygous for the Ca_v1.2 mutation (Ca_v1.2 DHP^{-/-}) had a DNA band at 475 bp; and heterozygous mice (Ca_v1.2 DHP^{+/-}) had a DNA band at both 390 bp and 475 bp.

2.2 Electrophysiology

All electrophysiological experiments in this thesis were carried out on transgenic mouse brain slices using the perforated patch clamp recording technique.

2.2.1 Slice preparation

Transgenic mice (2-4 months old) of either sex were deeply anesthetized with halothane and killed by chest compression. The skull was quickly opened to expose the brain, which was cooled *in situ* with ice-cold, carbogenated (95% O₂ and 5% CO₂) cutting

solution (composition: 250mM glycerol, 2.5 mM KCl, 1.2 mM NaH₂PO₄, 1.2 mM MgCl₂, 2.4 mM CaCl₂, 26 mM NaHCO₃, and 11 mM glucose, pH 7.4 when bubbled with carbogen). The brain was removed and a block containing the midbrain was cut horizontally on a Leica vibratome (VT 1000, Heidelberg, Germany). In order to restore normal cellular metabolism, tissue slices (300 µm thick) were allowed to recover at 32°C in carbogenated artificial cerebrospinal fluid (ACSF; composition: 126 mM NaCl, 2.5 mM KCl, 1.2 mM NaH₂PO₄, 1.2 mM MgCl₂, 2.4 mM CaCl₂, 26 mM NaHCO₃, and 11 mM glucose, pH 7.4 when bubbled with carbogen) for 40 min prior to recording. Slices were further trimmed to fit into a recording chamber and continuously perfused with carbogenated ACSF at a rate of 2-3 mL min⁻¹ at room temperature.

2.2.2 Nystatin-perforated patch clamp recording

Recordings were obtained using the perforated-patch technique to avoid artificial changes in the electrical properties of cells that can occur during conventional whole-cell recording. Nystatin was used as the pore-forming agent because this was found to produce reliable, long-lasting, stable recordings. The recordings were made within the confines of the VTA, as seen under differential interference contrast (DIC) and fluorescence microscopy. In fresh slices, the VTA is a semi-transparent area between the transparent, oval shaped substantia nigra.

Patch electrodes were prepared from glass micropipettes (Garner Glass, Claremont, California, USA, glass type KG-33, O.D. 1.5 mm, filament 0.10 mm) on a P-97 Brown-Flaming micropipette puller (Sutter Instruments, Novato, California, USA).

The tips of the patch pipettes were filled with intracellular solution (120 mM potassium acetate, 40 mM HEPES, 5 mM $MgCl_2$, and 0.5 mM EGTA with pH adjusted to 7.35 using 1 N KOH) then back-filled with the same solution containing $450 \mu g ml^{-1}$ nystatin and a pinch of Pluronic F127, yielding a tip resistance of 6-8 M Ω . While the intracellular solution could be stored in a refrigerator for weeks, the nystatin suspension was made fresh at the beginning of each week.

A small amount of positive pressure was applied to the pipette before it was advanced into the bath. Once submerged in the bath, the pipette offset was corrected to zero. Under DIC the pipette was positioned just above the VTA and slowly lowered down until a small dimple was seen on the cell of interest. A small negative pressure was applied to form a seal. High resistance seals (at least 1G Ω) were made using an Axon 700B amplifier. The signals were amplified and fed to a DigiData interface 1322A (Axon Instruments, Foster City, CA) driven by pClamp software (Axon Instruments, Foster City, California, USA)

It usually took 10-20 min for complete partitions of nystatin into the membrane. In current clamp mode, access was reflected by the size of the action potentials, as many VTA cells were spontaneously active. In voltage clamp mode, access was reflected by instantaneous current in response to a voltage change of -20 mV. After adequate access was attained, action potentials would overshoot 0 mV with an absolute size of at least 50 mV. Most recordings were of membrane voltages acquired in current clamp mode to study firing patterns of VTA cells and their modulation by LTCC modulators. Episodic protocols were also used in both voltage and current clamp mode to induce I_h and derive

other passive characteristics of the cell such as the current-voltage relationship and input resistance. Current and voltage pulses for I_h induction were of 1 sec duration and the intervals between pulses were 4 sec to allow complete recovery of H-channels. In voltage clamp mode the cell was held at -45 mV for maximum I_h induction. It was then brought to an initial level of -110 mV followed by 8 incremental steps of 10 mV. In current clamp mode, current was adjusted to hyperpolarize the cell to approximately -110 mV, followed by steps in increments of 20 pA.

Cells were identified based on whether or not they fluoresced green under 488 nm light. All cells that fluoresced green were considered DAergic (EGFP⁺) while all cells that did not fluoresce were considered non-DAergic (EGFP⁻, Figure 2.1).

Components of extracellular and intracellular solutions were purchased from bulk distributors Fisher Scientific (Nepean, Ontario, Canada) and VWR International (Mississauga, Ontario, Canada). All other chemicals were obtained from Sigma (St. Louis, Missouri, USA) and Tocris (Ellisville, Missouri, USA). Chemicals were dissolved in deionized water or DMSO (0.1% final concentration) as required. Aliquots of stock solutions were kept at -30°C. Prior to application, an aliquot was diluted to working concentration and applied to the ACSF bath. DA solution was made fresh daily with an equimolar concentration of the antioxidant disodium metabisulfite.

2.2.4 Data analysis

Data were analyzed offline with Mini Analysis (Synaptosoft Inc, Decatur, Georgia, USA) and pClamp software (Axon Instruments Inc, Foster City, California, USA). Basic

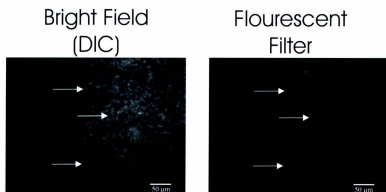


Figure 2.1: **Identifying the neurotransmitter content of VTA neurons.** Cells were initially identified under differential interference contrast microscopy (DIC; left frame) then exposed to 488 nm blue light under a flourescent filter (right frame). Cells containing EGFP protein flouresced green under the flourescent filter and were considered DAergic (arrow). Cells that were visible under DIC but not under the flourescent filter were considered non-DAergic.

properties of recorded cells such as action potential width, basal firing frequency, and resting membrane potential were averaged values of at least 1 min stable baseline recordings in current clamp mode. Action potential half width referred to the time difference between the rising and falling phases of an action potential at its half amplitude. I_h was measured as the difference in current between instantaneous and steady state readings. Analysis of firing behaviour was based on the interval between individual action potentials measured in the Mini Analysis program. Averaged, as well as instantaneous, firing frequencies were derived from those intervals. They were also used to express the regularity of action potentials and to detect burst firing, which was defined as more than two spikes in each burst separated by an inter-burst hyperpolarization. Bursts were quantified in two aspects: intra-burst frequency and inter-burst frequency. Intra-burst frequency is the averaged spike frequency within an individual burst, and inter-burst frequency is the frequency of the burst. Resting membrane potential referred to an average membrane potential where there was no firing, corrected for pipette offset. Afterhyperpolarization components were defined based on the following criteria (Figure 2.2; Koyama and Appel, 2006): fAHP (AHP-1): peak amplitude of AHP in less than 5 ms; mAHP (AHP-2): peak amplitude of AHP in 5-100 ms; and sAHP (AHP-3): peak amplitude of AHP in 100-300 ms. After recordings were complete and the cell was no longer required for further experiments pipette offset was measured and used to correct resting membrane potential values.

Data were expressed as mean \pm standard error of the mean as absolute values. Statistical comparisons were performed using either a two-tailed Student's *t*-test (paired

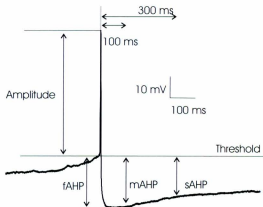


Figure 2.2: **The measurement of afterhyperpolarizations in VTA neurons.** Fast afterhyperpolarization (fAHP) is measured as the peak value within 5 ms following the action potential, medium afterhyperpolarization (mAHP) is measured as the peak value within 100 ms, and slow afterhyperpolarization (sAHP) is measured as the peak value within 300ms.

and unpaired where appropriate) or a two-way analysis of variance (ANOVA) and were considered significant when $p < 0.05$. For small sets where data points were too few to satisfy skew test, data were square root transformed before statistical analysis was conducted.

2.3 Immunohistochemistry

2.3.1 Transcardial Perfusion

Mice were deeply anesthetized with 0.1 ml (10 g/10 mL) chloral hydrate. A midline incision of approximately 3 cm was made from the sternal angle to the xyphoid process. The ribs were bilaterally cut and retracted to expose the heart. A small incision was made in the left ventricle close to the apex. A 21-gauge needle was used for perfusion. This needle was guided to the ascending aorta and was clamped in place for effective perfusion. The right atrium was cut to facilitate perfusion. Saline was perfused through the heart using a peristaltic perfusion pump (Master Flex, Thermo Scientific, Ontario, Canada) until the liver turned pale and outflow from the right atrium was clear. At this point, 4% paraformaldehyde in 0.1 M phosphate buffer was perfused for 20-25 min. The brain was then removed from the skull and left in 4% paraformaldehyde at 4°C for 1 hr before transferring to 20% sucrose in 0.1% phosphate buffer. The brains were left overnight at 4°C.

2.3.2 Sectioning

The fixed brains were frozen quickly by dry ice and 20 μm coronal sections were cut frozen using a cryostat at the level of the VTA -5.20 mm to -6.72 mm from Bregma. Every third section was collected, mounted onto gelatinized slides, and left to dry at room temperature. The slides were then used for immunohistochemistry.

2.3.3 Colocalization of EGFP and TH

To confirm the specificity of our mouse model, sections from EGFP^{+/+} mice were labeled with anti-TH primary antibody. The primary anti-TH mouse monoclonal antibody (Sigma, St. Louis, Missouri, USA) was diluted 1/200 in phosphate buffered saline (PBS) containing 2% TritonX-100, and 2% normal donkey serum. Sections were incubated in primary antibody overnight at 4°C. The slides were then rinsed in PBS 3 times for 5 minutes at room temperature and Alexa-594 conjugated donkey anti-mouse secondary antibody (Invitrogen, Ontario, Canada) was applied for 1 hour. Once again sections were rinsed 3 times for 5 minutes in PBS, then mounted with Vectashield mounting media (Vector Laboratories, Ontario, Canada) and coverslipped. Slides were stored in the dark at 4°C until analysis.

2.3.5 Image Analysis

2.3.5.1 Confocal Microscopy

Confocal microscopy was used to investigate the colocalization of EGFP and TH, in order to determine the specificity of our mouse model. The confocal microscope was equipped with blue (488 nm) and yellow (594 nm) lasers to visualize EGFP and Alexa-594 tagged TH cells, respectively. Quantification of positive immunoreactive cells was measured on confocal images by marking and counting color-coded cells using Image-J software (National Institutes of Health, USA). The percentage of DAergic cells not EGFP labeled was estimated as follows: $[1 - (\text{total colocalized TH}^+/\text{EGFP}^+) / (\text{total anti-TH labeled cells})] \times 100$. The percentage of non-DAergic cells labeled with EGFP was estimated as follows: $[1 - (\text{total colocalized TH}^+/\text{EGFP}^+) / (\text{total EGFP}^+ \text{ cells})] \times 100$. Six slices were collected from each animal, 2 each from the anterior, medial, and caudal portion of the VTA. All cells in each section were counted and an average overall colocalization was determined for each animal. Data were compared statistically with unpaired two-tailed Student's *t*-test and considered significant when $p < 0.05$.

Chapter 3 - Results

The VTA is a heterogeneous area that consists of DA and GABA containing projection neurons as well as GABA containing interneurons. Our setup allows us to see cells under DIC microscopy, however, DAergic and non-DAergic cells in the VTA cannot be distinguished based upon morphological properties. In order to accurately identify a cell's neurochemical phenotype, we acquired a mouse model with EGFP expression controlled by the TH promoter (Matsushita et al., 2002), thereby selectively expressing EGFP in DA containing cells of the VTA.

3.1 Genotyping Results

As homozygous expression of EGFP was lethal at postnatal day 21, the breeder pairs used to maintain this colony were heterozygous for EGFP. This meant a portion of the offspring were wild type with respect to EGFP expression and of no use to this study. After weaning, mice were genotyped and wild type mice were euthanized. Heterozygous EGFP mice (EGFP^{+/+}) had a DNA band at 582 bp, corresponding to the EGFP protein, while wild type mice (EGFP^{-/-}) had no visible DNA band (Figure 3.1A). Typically offspring of this mouse strain followed Mendelian estimates.

A second mouse strain was created, expressing both EGFP and a mutant Ca_v1.2 channel that carries a point mutation in the DHP binding site. Homozygous mice (Ca_v1.2DHP^{-/-}) had a DNA band at 475 bp, corresponding to the mutated calcium channel; wild type mice (Ca_v1.2DHP^{+/+}) had a DNA band at 390 bp, corresponding to

the normal calcium channel; and heterozygous mice ($Ca_v1.2DHP^{+/-}$) had both the 475 and 390 bp DNA band (Figure 3.1B).

Before patch clamp recordings were conducted, I examined whether there was an agreement between EGFP and TH expression. Immunohistochemistry was carried out to confirm the validity of the EGFP-expressing mouse model. $EGFP^{+/-}$ mice were sacrificed and immunolabelled for TH in order to quantify the amount of TH and EGFP colocalization (Figure 3.2). The EGFP has green fluorescence and the TH was labeled with Alexa-594. The colocalization rate, defined as the percentage of double positive cells (TH^+EGFP^+) in the total number of TH-positive cells, was used as measure of EGFP expression in DAergic neurons. The ectopic expression rate, defined as the percentage EGFP-positive but TH-negative (TH^-EGFP^+) cells in the total number of EGFP-positive cells, was used as an index of the frequency of EGFP expression in non-DAergic cells (Matsushita et al., 2002).

The average colocalization rate was found to be $90.97 \pm 1.39\%$ ($n=3$) indicating a strong agreement of EGFP and TH expression. However, an average of $11.81 \pm 3.00\%$ ($n=3$) of EGFP-positive cells did not show clear TH immunoreactivity (Figure 3.2). These results are consistent with previous reports of an 82.5% colocalization rate and 8.3% ectopic rate (Matsushita et al., 2002). In other words, although both EGFP and TH are controlled by the same promoter, there was almost 10% of TH-positive cells that did not have visible EGFP fluorescence and a similar number of EGFP-positive cells did not have visible TH-immunofluorescence.

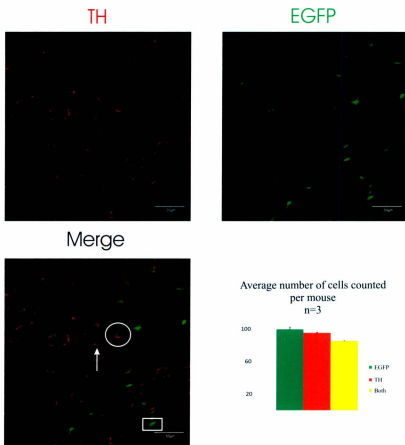


Figure 3.2: **Expression of EGFP in the VTA of the adult transgenic mouse.** TH signal (red), EGFP fluorescence (green), and their merged image are indicated. In the merged images, representative TH-EGFP-double positive (circle), TH-negative/EGFP-positive (square), and TH-positive/EGFP-negative (tip of arrow) are indicated. As seen in the merged image, EGFP is localized in various subcellular compartments, such as the nucleus, soma, and axon processes. Due to this, double labeled cells can be identified as having a green nucleus and red soma in the merged image. EGFP, enhanced green fluorescent protein; TH, tyrosine hydroxylase.

3.3 Electrophysiological results

Nystatin-perforated patch clamp recordings were made from 27 cells in the VTA. All cells were initially obtained in voltage clamp mode where the partitioning of nystatin into the membrane could be monitored by current injection. In the instance of spontaneously active cells, nystatin partitioning could be monitored in current clamp mode by action potential size. Cells which fluoresced green under 488nm light were considered DAergic (n=15); cells which did not fluoresce were considered non-DAergic (GABAergic, n=12).

3.3.1 Basic Electrophysiological Properties

In order to better understand the behavior and function of VTA neurons it is imperative to accurately identify whether a cell is DAergic or GABAergic. Based upon electrophysiological properties, criteria have been developed which distinguish DAergic and non-DAergic cells, predominantly focusing on DA autoinhibition and hyperpolarization induced inward current (I_h). The generally accepted fingerprinting is that DAergic cells respond to a DA receptor agonist with a strong hyperpolarization (inhibition) and display a large I_h current. Non-DAergic cells, on the other hand, do not respond to DA receptor agonist with inhibition and do not have a large I_h (Grace & Bunney, 1995; Grace & Onn, 1989). Other electrophysiological properties which vary between DAergic and non-DAergic cells in the VTA include, but are not limited to: basal firing rate, resting membrane potential, spike half width, and afterhyperpolarization profile. Classically, DAergic neurons are defined as having a slower basal firing rate,

more depolarized resting membrane potential, and longer spike half width when compared to non-DAergic neurons.

Recent studies have suggested that these criteria are better suited to describing subpopulations of DAergic and non-DAergic cells, and do not represent the properties of each cell type as a whole (Margolis et al., 2006; Zhang et al., 2010). In an attempt to corroborate the basic electrophysiological properties of cell populations in the VTA, I measured and compared the basic electrophysiological properties of DAergic and non-DAergic neurons of the VTA using a mouse model with EGFP labeled DAergic cells.

In vivo work by Grace and Bunney (1983) identified electrophysiological properties which set DAergic cells apart from non-DAergic cells of the SN and VTA. Primarily, they observed that DAergic cells are hyperpolarized in response to DA by activation of D₂ receptors, while GABA projection neurons and interneurons do not respond to DA with hyperpolarization. This hyperpolarization is dopamine receptor mediated autoinhibition. To investigate whether dopamine autoinhibition is exclusive to DAergic cells in the VTA, I measured the response of DAergic (green fluorescence) and non-DAergic (no fluorescence) cells to DA receptor agonist bath application (Figure 3.3). After a stable baseline recording of at least 5 minutes was obtained in current clamp mode, 50 μ M DA was bath applied for a maximum of 45 seconds and the change in firing frequency and membrane potential were recorded. DAergic cells displayed a clear hyperpolarization (n=15, pre: -53.01 ± 2.22 mV post: -64.25 ± 2.55 mV, $p < 0.05$ paired t-test, -10.4799 ± 1.838 mV average change) in response to 50 μ M DA application. This response was accompanied by a dramatic decrease in firing frequency in all spontaneously active

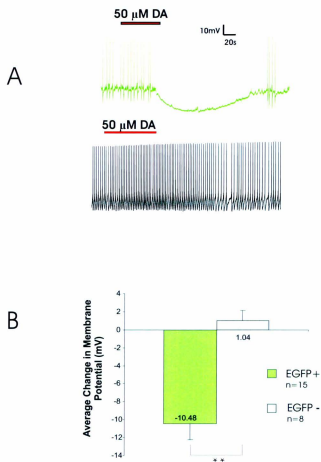


Figure 3.3: DAergic neurons display dopamine autoinhibition. **A)** Continuous current clamp recording from a representative DAergic (green) and non-DAergic (grey) cell showing the response to 50 μM dopamine bath application. **B)** Average change in membrane potential in response to 50 μM dopamine bath application. (** represents $p < 0.01$)

DAergic cells, with 60% of spontaneously active DAergic cells becoming silent and the remaining 40% decreasing in firing frequency by $58.14 \pm 22.18\%$. Hyperpolarization began after 42.70 ± 4.89 seconds of DA application with peak response occurring 88.77 ± 11.43 seconds after DA application. Cells returned to baseline levels after 125.26 ± 25.99 seconds of washout. Conversely, non-DAergic cells did not display hyperpolarization in response to $50 \mu\text{M}$ DA application ($n=8$, pre: -53.77 ± 2.45 mV, post: -52.88 ± 2.31 mV, $p > 0.05$ paired t-test, 1.038 ± 1.120 mV average change) and showed little change in firing frequency (average change: $-9.50 \pm 4.68\%$, $n=8$). The small change which did occur followed a similar time course as that of DAergic cells, with the initial response occurring at 38.51 ± 0.24 seconds, the peak response occurring at 68.12 ± 10.58 seconds, and a full recovery occurring at 114.5 ± 6.97 seconds following washout. When compared to each other, DAergic cells respond to $50 \mu\text{M}$ DA addition with significantly larger membrane hyperpolarization (-10.48 ± 1.74 mV vs. 1.04 ± 1.12 mV, $p < 0.01$, unpaired two-tailed t-test), and decrease in firing frequency (DAergic: $58.14 \pm 22.18\%$, non-DAergic: $-9.50 \pm 4.68\%$, $p < 0.05$, unpaired t-test).

3.3.1.2 DAergic cells have a larger I_h current

As previously discussed, the presence of a large magnitude hyperpolarization induced inward current is commonly used as a marker of DAergic neurons in the ventral midbrain. I wanted to determine whether this property is indeed only seen in DAergic neurons of the VTA. In voltage clamp mode, DAergic and non-DAergic cells were held at -45 mV, to ensure all H-channels were closed, before being hyperpolarized to -110 mV for 1 second. During the hyperpolarization pulse there was a gradual increase in inward

current seen in DAergic, but not non-DAergic cells. This was quantified by measuring the difference between the non-capacitance instantaneous current and steady state current (Figure 3.4A). DAergic neurons displayed a significantly larger I_h current than non-DAergic neurons (DAergic: -18.10 ± 6.12 pA, non-DAergic: -4.00 ± 0.88 pA, $p < 0.05$, unpaired two-tailed t-test, $n=6$ for both populations). This can also be seen in current clamp mode, where current injections are adjusted to result in a peak hyperpolarization of approximately -110 mV, causing an I_h "sag" to be visible on DAergic traces (Figure 3.4B).

3.3.2 Other fingerprinting criteria

3.3.2.1 Resting membrane potential and basal firing rate of DAergic and non-DAergic neurons are similar

During baseline conditions I measured the average resting membrane potential (RMP) of 13 DAergic and 10 non-DAergic neurons over a stable 5 minute period (Figure 3.5). A large overlap of RMPs was seen within the two populations, with DAergic RMPs ranging from -42.24 to -67.58 mV and non-DAergic RMPs ranging from -45.50 to -70.01 mV (average -52.22 ± 2.14 mV and -53.82 ± 0.66 mV, respectively, $p > 0.05$, unpaired two-tailed t-test).

Since RMPs are similar in DAergic and non-DAergic cells, and spontaneous firing is dependent on membrane potential, I next analyzed and compared basal firing frequency of DAergic and non-DAergic neurons. The average firing frequency of spontaneously active cells (73.3% of DAergic cells and 66.6% of non-DAergic cells) was measured during a stable 5 minute baseline recording (Figure 3.6). Although non-DAergic cells

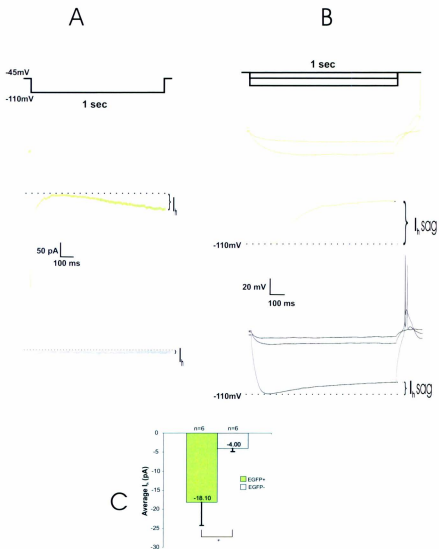


Figure 3.4: Hyperpolarization induced inward current (I_h) in VTA neurons. A) Voltage clamp recording showing a gradual increase in inward current in response to a voltage step to -110 mV for 1 second from a holding potential of -45 mV in DAergic (green) and non-DAergic (grey) neurons. B) Current clamp recordings showing a typical I_h “sag” for DAergic (green) and non-DAergic (grey) when current injections were adjusted to result in a peak hyperpolarization of about -110 mV. C) Quantitative analysis of I_h current in DAergic (green) and non-DAergic (grey) neurons. (* represents $p < 0.05$)

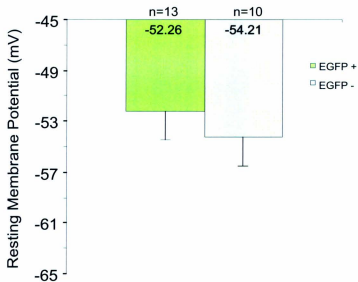


Figure 3.5: **DAergic neurons have a similar resting membrane potential as non-DAergic neurons.** Quantitative analysis of the resting membrane potential of DAergic (green) and non-DAergic (grey) neurons during baseline conditions.

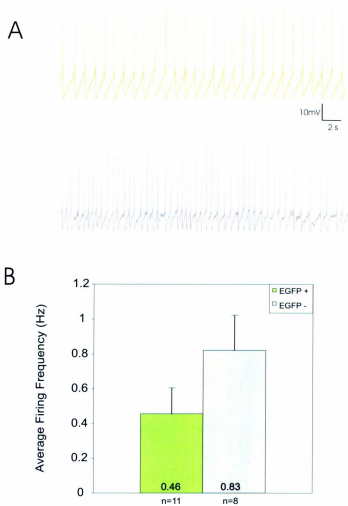


Figure 3.6: DAergic neurons appear to have a slower basal firing rate than non-DAergic neurons. A) Representative voltage clamp recording during baseline conditions for a spontaneously active DAergic (green) and non-DAergic (grey) neuron. B) Quantitative analysis of basal firing rate of DAergic and non-DAergic neurons during baseline conditions.

had a tendency to fire at a higher frequency, there was no statistical difference in basal firing rates (DA, n=11, 0.456 ± 0.283 Hz; non-DA, n=8, 0.826 ± 0.359 Hz; $p > 0.05$, unpaired two-tailed t-test). There is, however, a distinct difference in the action potential and AHP profile of DAergic and non-DAergic neurons.

3.3.2.2 Spike and afterhyperpolarization profile vary between DAergic and non-DAergic neurons

During the same 5 minutes of stable baseline recording used to determine RMP and basal firing rate, AHPs and spike half width were measured and compared for 5 DAergic and 4 non-DAergic neurons. During baseline conditions, the medium and slow component of AHPs (mAHP and sAHP, respectively) are significantly larger in DAergic cells (mAHP: -10.76 ± 1.60 pA; sAHP: -7.66 ± 1.01 pA) than non-DAergic cells (mAHP: -6.22 ± 1.23 pA; sAHP: -2.19 ± 0.62 pA, $p < 0.05$, unpaired two tailed t-test), while the fAHP was similar (DAergic: -12.08 ± 1.63 pA; non-DAergic: -11.31 ± 0.60 pA, $p > 0.05$, unpaired two tailed t-test; Figure 3.7).

Similarly, spike half width duration of both cell populations was significantly different during baseline conditions (Figure 3.8). DAergic cells had a significantly longer action potential duration (DAergic: n=13, 2.92 ± 0.27 ms vs. non-DAergic: n=9, 1.94 ± 0.17 ms, $p < 0.05$ unpaired two-tailed t-test). However, there is overlap in the range of half widths measured, 1.14 to 4.60 ms in DAergic neurons, and 1.08 to 2.71 ms in non-DAergic neurons, negating the possibility of using this criterion exclusively to identify a cell's neurotransmitter identity.

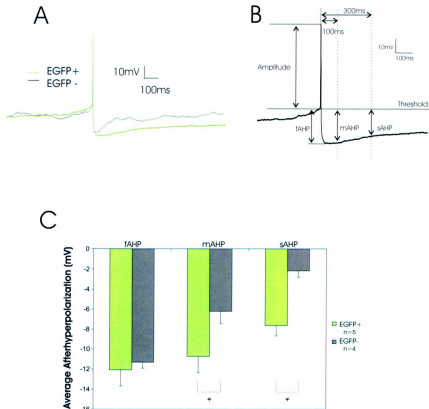
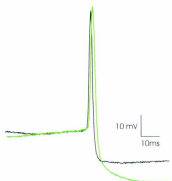


Figure 3.7: Afterhyperpolarization profiles of DAergic and non-DAergic neurons. A) Representative single spike during baseline conditions for a spontaneously active DAergic (green) and non-DAergic (grey) neuron. B) Time course for each of the three afterhyperpolarizations (AHPs) C) Quantitative analysis of the AHP profile of DAergic (green) and non-DAergic (grey) neurons. (* represents $p < 0.05$) fAHP, fast afterhyperpolarization; mAHP, medium afterhyperpolarization; sAHP, slow afterhyperpolarization.

A



B

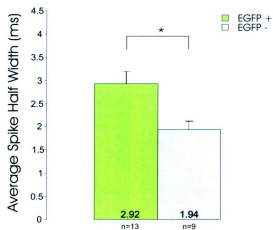


Figure 3.8: DAergic neurons have a longer duration action potential than non-DAergic neurons. A) Representative current clamp recording from a spontaneously active DAergic (green) and non-DAergic (grey) neuron. B) Quantitative analysis of average spike half width of DAergic (green) and non-DAergic (grey) neurons. (* represents $p < 0.05$)

3.3.3 LTCC modulation

Following analysis of the basic intrinsic properties of DAergic and non-DAergic neurons I wanted to investigate the role LTCCs play in firing pattern modulation of both cell groups. While previous work from our lab demonstrated that LTCC activation induces burst firing in DAergic neurons, the role of LTCCs in non-DAergic firing pattern modulation remains unknown.

3.3.3.1 FPL 64176 can induce burst firing in DAergic and non-DAergic neurons

After a stable baseline recording was established for at least 5 minutes, 1 μM of the LTCC activator FPL 64176 was bath applied to slices for 12-13 minutes and the response was measured. A similar depolarization was evoked in DAergic and non-DAergic neurons (3.67 ± 0.79 mV vs. 4.56 ± 0.54 mV, respectively, $n=11$ in both populations, $p>0.05$, unpaired two-tailed t-test, Figure 3.9). This depolarization led to a change in firing frequency and pattern in both cell populations. The firing frequency of 45.6% (5/11) of DAergic and 36.4% (4/11) of non-DAergic cells increased but remained in the single spike firing pattern in response to 1 μM FPL 64176. This response began 18.53 ± 3.41 minutes after FPL 64176 addition began and peaked 31.61 ± 3.53 minutes after FPL addition in both populations. Single spike firing was converted to burst firing in 36.4% (4/11) of DAergic and 45.6% (5/11) of non-DAergic cells. A change in firing typically began 16.25 ± 2.81 minutes after FPL addition and a peak response was seen 23.64 ± 4.11 minutes after FPL addition. (Figure 3.10 and 3.11). This change in the firing pattern returned to baseline levels after considerable washout time (hours). No change in

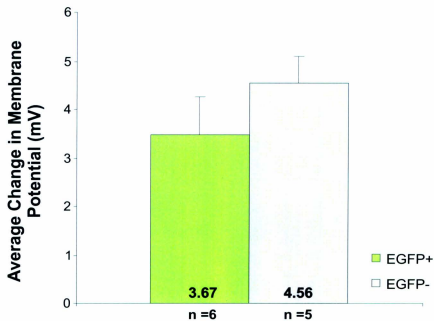


Figure 3.9: Average change in resting membrane potential in response to 1 μ M FPL 64176. DAergic (green) and nonDAergic (grey) neurons respond to the LTCC agonist FPL 64176 with similar depolarization.

the firing pattern or frequency was seen in 2 cells from each group. These cells also showed the smallest depolarization in response to FPL 64176 addition.

To confirm that LTCC modulation is responsible for the change in firing pattern observed after 1 μM FPL addition, 10 μM of the LTCC antagonist nifedipine was bath applied to 4 bursting cells (2 DAergic and 2 non-DAergic). 4.76 \pm 2.24 minutes after nifedipine addition the burst firing pattern was converted to single spike firing in all cells (Figure 3.10 and 3.11). Washout of nifedipine resulted in burst firing resuming and remaining for several hours.

3.3.3.2 mAHP changes during baseline, bursting, and return to single spike

In an effort to better understand the transition of single spike firing to burst firing, I compared various spike properties during FPL 64176 induced bursting to baseline values. Action potential half width remained constant during burst firing, however there was a decrease in mAHP size during burst firing in both DAergic (-13.70 \pm 0.80 mV baseline, -5.28 \pm 0.38 bursting, n=2) and non-DAergic cells (-20.74 \pm 0.49 mV baseline, -9.60 \pm 2.05 mV bursting, n=2). This decrease in mAHP allows a train of APs to be fired in quick succession. The mAHP returned to near baseline levels (-13.72 \pm 0.56 mV and -13.24 \pm 1.97 mV) after nifedipine addition converted burst firing to single spike firing. During bursting, the sAHPs of multiple APs summate following the burst, creating a large sAHP tail. When DAergic and non-DAergic AHPs were pooled (Figure 3.12), mAHP significantly decreased during burst firing (-17.22 \pm 1.83 mV, baseline and -7.44 \pm 2.12 mV, bursting, n=4, p<0.01, unpaired t-test) and significantly increased, to near

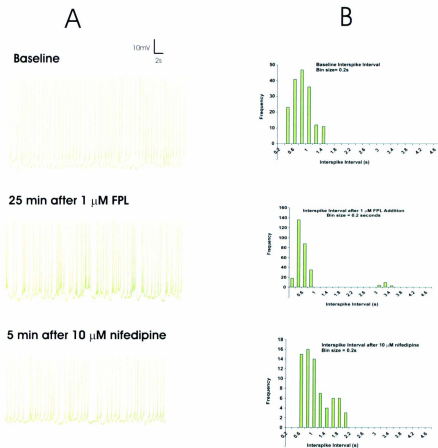


Figure 3.10: **FPL 64176 induces burst firing of VTA DAergic neurons.** A) Current clamp recording of a representative cell showing the LTCC agonist FPL 64176 converted regular single spike firing to burst firing and the LTCC antagonist nifedipine converted burst firing to single spike firing. B) Interspike interval (ISI) plot in 200 ms bins in control conditions (top), after FPL 64176 addition (middle) and after nifedipine addition (bottom). FPL 64176 dramatically shifted the primary peak to the left and gave rise to a secondary peak corresponding to the frequency of bursting cycles.

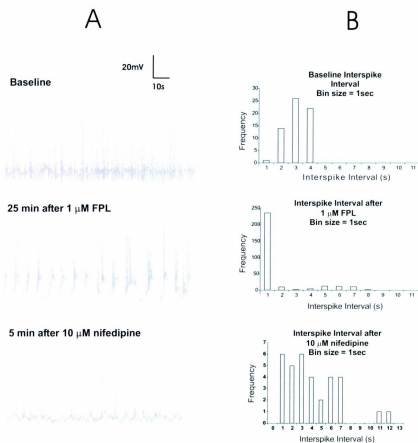


Figure 3.11: FPL 64176 induces burst firing of VTA non-DAergic neurons. A) Current clamp recording of a representative cell showing the LTCC agonist FPL 64176 converted regular single spike firing to burst firing and the LTCC antagonist nifedipine converted burst firing to single spike firing. B) Interspike interval (ISI) plot in 1 second bins in control conditions (top), after FPL 64176 addition (middle) and after nifedipine addition (bottom). FPL 64176 dramatically shifted the primary peak to the left and gave rise to a secondary peak corresponding to the frequency of bursting cycles.

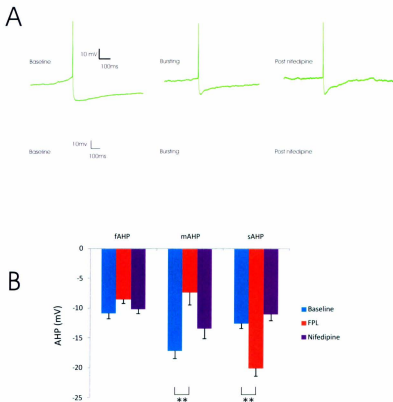


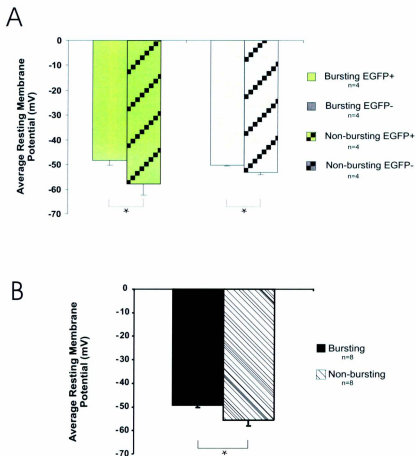
Figure 3.12: The afterhyperpolarization profile of DAergic and non-DAergic neurons changes during burst firing. A) Representative current clamp trace of a DAergic (green) and non-DAergic (grey) neuron, that responded to FPL 64176 with burst firing, during baseline, FPL 64176 induced burst firing, and nifedipine induced single spike firing. B) Quantitative analysis of the change in afterhyperpolarization (AHP) profile of cells that responded to FPL 64176 with burst firing. There is a significant decrease in medium AHP (mAHP) during FPL induced burst firing. After nifedipine restores single spike firing the mAHP returns to near baseline values. During burst firing sAHP was measured as the post burst tail. (** represents $p < 0.01$)

baseline values, following nifedipine (-7.44 ± 2.12 mV, bursting and -13.48 ± 1.00 mV, post nifedipine, $n=4$, $p < 0.01$, unpaired t-test).

3.3.3.3 Baseline properties and LTCC mediated burst firing

Since both DAergic and non-DAergic cells responded to an LTCC activator with increased firing and bursting, I examined what was common to bursting cells in both groups. If cells are grouped based upon their response to the LTCC modulator FPL 64176, both DAergic and non-DAergic cells with a more depolarized resting membrane potential during baseline conditions were those that responded to the LTCC opener with burst firing (Figure 3.13). This is not simply a matter of depolarized membrane potential alone, as injecting current into a spontaneously inactive, non-bursting cell results in an increased firing rate, but it remaining in the single spike firing pattern. If the same current is injected after LTCC agonist application, however, burst firing occurs (not shown). Not surprisingly, the cells that respond to the LTCC agonist with burst firing have a significantly larger FPL 64176 induced depolarization than non-bursting cells (5.06 ± 0.39 mV bursting, 3.32 ± 0.31 mV non-bursting, $p < 0.05$, unpaired two-tailed t-test).

During baseline conditions, the cells that responded to LTCC agonist with burst firing had a larger mAHP than cells that did not respond with burst firing (bursting: -18.78 ± 1.29 mV, non-bursting: -8.41 ± 1.39 mV). mAHP was reduced after FPL 64176 addition in both cell populations (bursting: -9.721 ± 1.49 mV, non-bursting: -6.21 ± 2.53 mV). This change in mAHP size was significant in bursting cells (baseline: -18.78 ± 1.29 mV, FPL: -9.72 ± 1.49 mV) but not non-bursting cells. Similarly, addition of the LTCC



antagonist nifedipine returned mAHPs to near baseline values (bursting: -13.36 ± 0.67 mV, non-bursting: -5.50 ± 0.42 mV), a change that was significant in bursting cells (FPL: -9.721 ± 1.49 mV, nifedipine: -13.36 ± 0.67). The sAHP is also dramatically changed during burst firing. Bursting cells develop a large post-burst hyperpolarization after FPL 64176 addition which returns to near baseline levels following nifedipine addition (baseline: -14.20 ± 1.14 mV, FPL: -20.72 ± 2.31 mV, and nifedipine: -12.31 ± 1.91). Non-bursting cells do not display this change in sAHP (baseline: -5.39 ± 1.22 mV, FPL -6.13 ± 0.41 mV, and nifedipine: -2.29 ± 0.16 mV).

AHP profiles (fAHP, mAHP, and sAHP) were analyzed using a two way ANOVA with treatment (baseline, FPL 64176, nifedipine) and bursting (burst or non-burst cells following LTCC activation) as factors followed by Schelle post hoc test. For fAHP, there was no significance for treatment or bursting. For mAHP and sAHP, treatment as a factor showed a significant difference. Post-hoc analysis indicates a significant difference between baseline and FPL 64176 and also between FPL64176 and nifedipine, however, there was no difference between baseline and nifedipine. When cells were grouped as bursting or non-bursting following LTCC activation and used as a factor, it showed a significant difference in mAHP and sAHP. During baseline conditions, the mAHP of cells that went on to burst fire was significantly larger than the mAHP of cells that did not burst fire. After FPL 64176 the mAHP and sAHP of bursting cells changed significantly, and returned to near baseline levels following the application of nifedipine. Non-bursting cells had a small but nonsignificant change in m- and sAHP. Moreover, there was a

significant interaction between the two factors, suggesting drug treatment affected bursting cells more than non-bursting cells (Figure 3.14).

3.3.4 LTCC subtype involvement

By crossing the previously established EGFP transgenic mouse strain with a mouse strain containing a mutation in the DHP binding site of the Ca_v1.2 subtype (Striessnig et al., 2006) I could investigate and compare which LTCC subtype is responsible for modulating firing patterns in DAergic and non-DAergic cell populations of the VTA. The point mutation rendered the DHP binding site of Ca_v1.2 inactive, thereby allowing me to selectively target each LTCC subtype. Drugs working through DHP binding (i.e., (S)-(-)-Bay K8644 and nifedipine) only modulate the Ca_v1.3 channel, while those working through the benzopyrrole site (i.e., FPL 64176) modulate both Ca_v1.2 and Ca_v1.3. After a stable 5 min baseline recording 1 μ M FPL 64176 was bath applied to 2 DAergic and 2 non-DAergic cells. A change in the firing pattern was seen in all cells approximately 15 minutes after FPL addition, with a peak burst firing response seen approximately 20-25 minutes after application. 10 μ M nifedipine bath applied for 5-7 minutes converted FPL induced bursting to single spike firing, which returned to burst firing following nifedipine washout (Figure 3.15). This response to Ca_v1.3 modulation was seen in DAergic and non-DAergic cell types, suggesting Ca_v1.3 is important for modulating firing patterns in both cell populations. Similarly, bath application of 5 μ M (S)-(-)-Bay K8644 induced burst firing in both DAergic and non-DAergic cells (n=2 for both) within 20 minutes after application, and burst firing returned to single spiking after

prolonged washout (not shown). While the sample size is small, it does indicate that $Ca_v1.3$ is responsible for bursting in DAergic and non-DAergic cells.

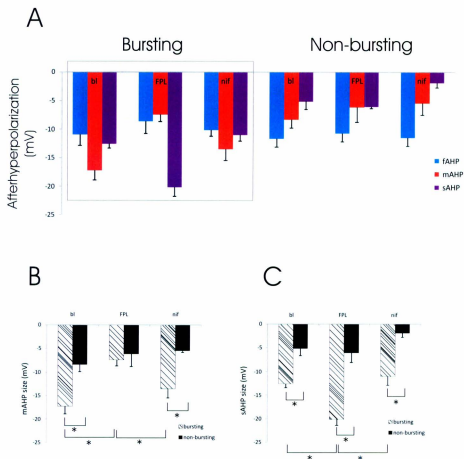


Figure 3.14: Afterhyperpolarization profile during baseline conditions is related to FPL 64176 induced burst firing. A) The AHP profile of bursting and non-bursting neurons. For simplicity significance bars have been omitted. B) Cells with a larger mAHP and C) sAHP during baseline conditions were the neurons which responded to the LTCC agonist FPL 64176 with burst firing. During burst firing mAHP and sAHP is changed significantly from baseline values. sAHP was measured as the post burst tail. Bursting $n=4$, non-bursting $n=4$ (* represents $p<0.05$ using a two way ANOVA and Scheffe post-hoc test) AHP, afterhyperpolarization; bl, baseline; FPL, after FPL application; nif, after nifedipine application.

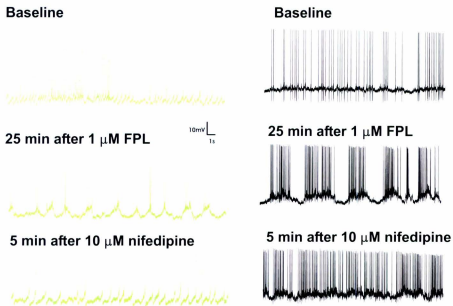


Figure 3.15: **Ca_v1.3 is responsible for modulating burst firing in DAergic and non-DAergic neurons.** Using a mouse model with DHP insensitivity in the Ca_v1.2 channels, Ca_v1.3 could be selectively modulated in DAergic (green) and non-DAergic (black) neurons. FPL 64176 opens both LTCC subtypes, while nifedipine blocks only Ca_v1.3 channels. When Ca_v1.3 channels are selectively blocked, burst firing converts to single spike firing.

Chapter 4 - Discussion

In this thesis, we observed variations in basic electrophysiological properties between DAergic and non-DAergic neurons of the VTA, distinguished based upon the presence or absence of EGFP driven by the TH-promoter. DAergic and non-DAergic neurons responded to an LTCC agonist with a change in firing rate and in some cells a switch of firing pattern from single spike firing to bursting. The tendency to burst fire was correlated to resting membrane potential and AHP profile during baseline conditions. Here we discuss our results in two main parts, basic electrophysiological properties and LTCC modulation, with a brief discussion of technical considerations including the animal model employed for all experiments.

4.1 Technical considerations

4.1.1 Recording method used

A major technical consideration relevant to this project is the patch clamping method used. The perforated patch clamp technique used in this work has a number of advantages over conventional whole cell intracellular recording. The channels formed by nystatin are small and impermeable to molecules larger than glucose; typically only small ions such as Na^+ , K^+ , and Cl^- can pass through. Therefore, recordings can be made without dialyzing important substances of small molecular weight from the cytoplasm. Consequently, currents run down significantly more slowly and second messenger cascades and mechanisms important to cell signaling and channel regulation are kept

operative (Fu et al., 2003). Of particular importance to the work of this thesis is the lack of calcium rundown during nystatin perforated patch clamping. A major component of this thesis was examining the effect of LTCC modulation on firing patterns. As shown in previous work, LTCC induced bursting is dependent on calcium and intracellular signaling molecules such as PKC (Liu et al., 2007), which are easily dialyzed during conventional whole cell recording but remain intact during perforated patch clamp recording. Since nystatin forms channels in the membrane, instead of rupturing a small section of membrane as in conventional whole cell patch clamping, the access resistance is higher. Even in the case of the most efficient nystatin perforations, access resistance will be higher than in conventional whole cell recording. For the majority of experiments conducted in this thesis a slightly higher access resistance was irrelevant because the primary readout was action potentials. This only became a point of interest during I_h protocols, where the membrane potential of the cell was being manipulated to specific levels. An increased access resistance would cause a portion of the current injection to be lost, thereby hyper- or depolarizing the cell less than expected, inducing a smaller I_h as reported in this thesis. In consideration of this, access resistance was closely monitored and cells used in this study had an average access resistance of $58.42 \pm 15.17 \text{ M}\Omega$. It is important to note however, that the higher access resistance innate to the perforated patch clamp method had no effect on firing pattern analysis.

4.1.2 Recording conditions

When considering the discrepancies of our values from other reported values, it is important to remember the effect of temperature on ion channel function. Often

recording takes place at temperatures close to body temperature (37°C); all recordings in this thesis took place at room temperature (22°C). This temperature was used in an effort to prolong cell viability and avoid cellular death before an experiment was complete. Temperature regulates the rates of enzyme catalyzed reactions and affects the function of ion channel proteins. For example, I_h is found to be more conductive at higher temperatures (Vargas & Lucero, 1999). As well, LTCCs are found to be more conductive, have more hyperpolarized activation voltages, and an accelerated recovery from inactivation at temperatures between 36-37°C when compared to lower temperatures between 21-23°C (Huneker et al., 2004; Peloquin et al., 2008). The temperature sensitive reduction in I_h efficiency and LTCC activity is reflected in this study. I_h measurements and firing frequency of DAergic and non-DAergic cells are lower in this study than commonly reported by other groups at higher temperatures. Similarly, the activity of cells between mice and rats, while essentially the same, can have small discrepancies. A rat's body temperature is typically 37°C while a mouse has a body temperature of 39°C, giving rise to a bigger differential temperature when recordings take place at 22°C.

Additionally, the age of the animal has been shown to influence firing rates and patterns. A small number of DAergic cells in slices of pre-weaning aged rats and mice spontaneously burst fire, which is not seen in adult slices. It is believed that firing pattern regulation is under different control in the juvenile DAergic cells. Adult DAergic cell pacemaking is under LTCC control, while juvenile DAergic cells rely on Na^+/HCN channel control (Chan et al., 2007). As discussed in Chapter 1, spontaneous burst firing is commonly seen in DAergic neurons *in vivo* while it is rarely seen *in vitro*.

Spontaneous burst firing has, however, been reported in a small portion (18.3%) of DAergic neurons in brain slices from juvenile (15-21 day old) rats (Mereu et al., 1997). It appears this spontaneous burst firing is attributable to NMDA receptor activation, as the spontaneous bursting ceases when NMDA receptor sensitivity declines with age. NMDA receptor activation also induces burst firing in adult animals, although a hyperpolarizing current is required for this induction (Overton et al., 1997). Therefore, when comparing results in this thesis to results of other groups, animal age and species are important considerations, as this thesis contains data obtained exclusively from adult mice two to six months of age.

4.1.3 Animal model

All experiments in this thesis used a mouse model new to our lab. A colony of EGFP expressing mice also carrying a Ca_v1.2 point mutation was initially difficult to establish. Eventually a population of EGFP^{+/+}/Ca_v1.2DHP^{-/-} breeders were established and the colony was easily maintained. The litter sizes (not recorded but passively observed) were often smaller than those of EGFP^{+/+}/Ca_v1.2DHP^{+/+} mice, and EGFP^{+/+}/Ca_v1.2DHP^{-/-} mice destroyed their litters more often than EGFP^{+/+}/Ca_v1.2DHP^{+/+} mothers. As well, we encountered a stretch of 4-5 months where construction work was underway next to the animal facility which disrupted breeding. In an effort to increase frequency and survival of litters we began pairing 1 male per 2 females, allowing both females to care for each litter and thereby increasing pup survival rates. Although we encountered occasional breeding problems the age of animals used for experiments remained constant.

The exposure of cells containing EGFP to 488 nm light was tightly controlled to avoid possible negative effects of excited EGFP within DAergic cells. Early in our experimental work, while setting up and testing the animal model, we noticed EGFP⁺ (DAergic) cells exposed to 488 nm light became very fragile and died faster than their EGFP⁻ (non-DAergic) neighbours. Prior to the start of recordings cells were briefly exposed to 488 nm light in order to determine their identity. Once recording was completed and the slice was no longer required for future experiments the fluorescent filter was applied and the cell identity re-confirmed, this time with no time limit for light exposure.

Due to the method of identification used, I feel all cells were identified correctly and did not suffer any ill effects of EGFP excitation. Occasionally the fluorescence of the cell was difficult to distinguish from the background; some slices fluoresce stronger than others. These cells were not included in analysis.

4.1.3.1 EGFP driven by the TH promoter efficiently labels DAergic neurons

The findings of this thesis are contingent on the accuracy of the animal model used. The typical and ectopic expression frequency of EGFP agree with the values reported by the group that created this strain (Matsushita et al., 2002), and are better than expression frequencies reported by other groups using a similar model (Zhang et al., 2010). Our model provides accurately labeled DAergic cells, with $90.97 \pm 1.39\%$ of DAergic cells labeled with EGFP. Interestingly, $11.81 \pm 3.00\%$ of non-DAergic are also labeled with EGFP. This group of EGFP⁺/TH⁻ cells, as determined by

immunohistochemistry, may represent a population of cells that are expressing TH at levels below our detection threshold. Considering EGFP is driven off of the TH promoter in our model, it is highly unlikely that cells not expressing TH would be expressing EGFP. The transcription of EGFP is contingent on TH transcription, and it can be assumed that if the EGFP gene is transcribed, the TH gene is also transcribed. Of particular importance is the fate of these two protein products: TH is metabolically active while EGFP is poorly degraded. During times of increased cellular activity TH and EGFP levels will increase; however, during times of decreased cellular activity TH will be degraded but EGFP will remain. Imagine a DAergic cell is active during early development (maybe up to PND 30) then not active again at any point during the 60 days before the animal is sacrificed. Given TH has an estimated half life of 64 – 72 hours (Gahn & Roskoski, 1995), during the 2 months of inactivity all TH will be degraded but EGFP will remain. With this in mind, it is possible TH⁺/EGFP⁺ cells represent a population of cells whose activity has changed. Conversely, a cell that has recently become active will generate TH but will have lower EGFP levels (TH⁺/EGFP⁻) than a cell that has been active longer and thus been producing EGFP longer. For example, consider the EGFP produced by a cell that has been active for 90 days compared to the EGFP produced by a cell that has only been active for the previous 7 days. If the detection of TH and EGFP could be optimized it is very likely the ectopic expression frequency would decrease. Overall, our model provides a reliable method for identifying DAergic and non-DAergic cells *in vitro*. When compared to the dependability of other cell identification methods, such as post hoc immunohistochemistry, single cell reverse-transcription polymerase chain reaction (RT-

PCR), and electrophysiological fingerprinting, the model we chose, while not an unequivocal index, provides a reliable method of cell identification.

4.1.3.2 EGFP vs. other means of identifying cells

Identifying cells based on post hoc immunohistochemistry presents many challenges. Most importantly, this method requires the use of conventional whole cell patch clamping in order to allow the cell to be labeled with a marker such as Lucifer yellow or neurobiotin. After a lengthy recording time using conventional whole cell access, the possibility of dilution or rundown of the molecule of interest (i.e., TH as a DAergic label) is possible, increasing the likelihood of false negatives. There are also limitations associated with single cell RT-PCR in order to identify cell types. Care must be taken to avoid contamination of the pipette tip while it is being lowered into the slice. Given that the premise of RT-PCR is to amplify the mRNA of interest, contamination of the pipette tip may result in false positives. Similarly, care must be taken to maintain an RNase free environment in order to avoid degradation of the mRNA, resulting in false negatives. During long duration whole cell recording there is a potential for RNA degradation, confounding the technical issues often encountered in PCR protocols. Moreover, both post recording identification methods are considerably more time consuming than cell identification using the EGFP mouse model. Specific cell populations can easily be targeted using our transgenic mouse model with high reliability.

There has been much debate over the validity of electrophysiological fingerprinting as a method of cell identification. While multiple groups have shown

certain properties to be unique to one cell type, recent reports have suggested a much larger overlap of electrophysiological properties, suggesting 'putative' cell populations are actually subpopulations within a cell type, or a mixture of cell types (Margolis et al., 2006; Lammel et al., 2008; Zhang et al., 2010). Due to its convenience to employ and previously supported accuracy, this method of cell identification is commonly used *in vivo* and *in vitro*.

4.2 Basic electrophysiological properties

Using what we feel to be a reliable cell labeling system, we investigated various basic electrophysiological properties in DAergic and non-DAergic cell populations. These findings will be discussed in detail.

The original criteria (Grace et al., 1989) developed in rat midbrain slices define non-DAergic cells (TH negative immunohistochemistry) as having short duration action potentials (less than 1.5ms), high firing frequencies (greater than 10Hz) and phasic or burst firing patterns. Conversely, DAergic cells (TH positive immunohistochemistry) are described as having spontaneous pace-maker like depolarizing potential, a highly regular firing pattern, long duration (greater than 2 ms) action potentials, and a high (depolarized) spike threshold. Spontaneously active DAergic cells recorded *in vitro* had similar electrophysiological characteristics in common with those of DAergic neurons recorded *in vivo*; however, *in vitro* DAergic cells exhibited substantially higher input resistance and fired in a very regular pacemaker pattern, with no spontaneous burst firing (Grace et al., 1989). These experiments provide initial evidence for identification of DAergic

neurons in the *in vitro* brain slice preparation, which has been supported by numerous groups over the past two decades (Grace et al., 1989; Johnson & North, 1992b; Neuhoff et al., 2002). More recently, it has been suggested that these criteria oversimplify the properties of each cell population and lead to identification of subpopulations within each cell type. For example, Margolis and colleagues identify a population of TH negative cells having an I_h of comparable size to TH positive cells, as well as a population of TH positive cells which are unresponsive to D2 receptor agonists (Margolis et al., 2006). Similarly, Lammel and colleagues suggest molecular and physiological differences within the DAergic cell group (Lammel et al., 2008). They suggest not all DAergic neurons express the same receptors nor do they share the same electrophysiological properties.

4.2.2 DA autoinhibition is only seen in DAergic cells of the VTA

Although D2 receptors are expressed by both DAergic and non-DAergic neurons (Bouthenet et al., 1987; Chen et al., 1991), DA agonist affects each cell type differently. As outlined in Chapter 1, D2 receptors are coupled to GIRK channels and upon activation induce a membrane hyperpolarization. Consistent with previous reports, DAergic, but not non-DAergic cells, responded to a DA receptor agonist with hyperpolarization (Margolis et al., 2006; Grace et al., 1989; Grace & Bunney, 1983; Steffensen et al., 1998). Moreover, in this study, hyperpolarization resulted in a complete cessation of spontaneous firing in 60% of DAergic cells. Contrary to some reports, all DAergic neurons in this study responded with strong hyperpolarization. Work by both Lammel et al and Margolis et al suggest that there is a subpopulation of DAergic neurons, clustered in the medial VTA, projecting to the PFC which do not express D2 autoreceptors and

therefore show no response to DA agonists (Lammel et al., 2008; Margolis et al., 2006). This cell population was not seen in this study, most likely due to the fact specific regions of the VTA were not targeted. Instead, this work treated the VTA as a homogeneous region and targeted the healthiest cells in the VTA, regardless of their location within the VTA borders. Due to the relatively small sample size in this thesis it is probable no DAergic cells were sampled from the paranigral nucleus discussed in previous work. Similarly, no non-DAergic neurons in this study responded to DA application with strong hyperpolarization, although the presence of a small population of non-DAergic neurons hyperpolarizing in response to DA agonists have been previously reported (Margolis et al., 2006; Yim & Mogenson, 1980). GABAergic neurons of the VTA do not express D2 autoreceptors, conversely, a population of GABAergic cells has been shown to increase firing in response to DA application (Stobbs et al., 2004). GABAergic neurons couple electrically via connexin-36 gap junctions in response to DA application (Lassen et al., 2007) and this response is restricted to GABA neurons in the VTA. Based upon the findings of this thesis, DA autoinhibition is specific to DAergic neurons.

4.2.4 I_h current

When compared to previous reports, the I_h values recorded in this work are smaller than anticipated. Typically DAergic neurons display I_h currents of >100 pA while non-DAergic neurons have a significantly smaller I_h (Grace et al., 1989; Margolis et al., 2006; Zhang et al., 2010). As discussed above, the technical limitation of nystatin perforated patch clamp may be partially responsible for the lower than expected I_h values seen in this work. As I_h is measured after a pulse is injected, a higher access resistance

will result in an error in voltage clamp. Similarly, a higher access resistance would result in a portion of the I_h current being lost, making it seem smaller than it really is. Also, H-channels are distributed all over the cell body. In order to activate all of these channels full access is necessary. In the case of partial access only the channels in the immediate vicinity of the electrode are activated and only those channels will be contributing to the I_h current measurements. It is also important to remember that I_h is temperature sensitive, that is H-channels are less conductive at lower temperatures. While many groups record at temperatures near body temperature, all of our recordings are at room temperature. However, temperature is most likely not a major factor in the lower than anticipated I_h currents recorded in this work, as very large I_h has previously been recorded in DAergic cells at room temperature (Zhang et al., 2005; Liu et al., 2007). It should be noted that although the magnitude of I_h was lower than expected, the trend observed suggests I_h is larger in DAergic neurons. This suggests there was an intrinsic technical problem present in all I_h recordings, most likely incomplete access at the time of I_h recordings.

4.2.5 Afterhyperpolarization profile

Examining the AHP profile of DAergic and non-DAergic neurons during baseline conditions provides an explanation of many other basic electrophysiological properties seen in this thesis. As outlined in Chapter I, the expression and activity of many intrinsic channels influence the firing pattern and activity of a cell. In the case of DAergic and non-DAergic cells in the VTA the difference in intrinsic channel expression and activity can be seen in analysis of afterhyperpolarization potentials, which themselves shape cellular properties during baseline conditions. For example, since DAergic neurons have

a larger slow and medium AHP during baseline conditions it makes sense that basal firing rates would be slower. DAergic neurons are taking longer to return to resting membrane potential after each action potential, increasing the time between APs. sAHP is shaped by the M- and H-channels (Koyama et al., 2006; Neuhoff et al., 2002) while the mAHP is shaped by SK channel activity (Bond et al., 2004). Analysis of AHPs suggests M-channel activity is greater in DAergic cells, while SK channel activity is lower in DAergic neurons.

Most groups report spontaneous firing rates during baseline conditions to be higher than the values reported in this work. This may be due to previously discussed technical considerations, mainly temperature, as higher access resistance would not affect spontaneous firing rate.

Similarly, resting membrane potential under baseline conditions is slightly different than previously reports. Previous classifications have identified DAergic resting membrane potentials near -60 mV and non-DAergic resting membrane potentials near -70 mV (Johnson et al., 1992b). The work of this thesis identifies DAergic neurons sitting at slightly more depolarized resting membrane potentials, however there is a great amount of overlap between the two groups (average DAergic: -52.22 ± 2.14 mV and non-DAergic: -53.82 ± 0.66 mV) and is not able to be used as a distinguishing feature.

4.2.6 Spike half width

A commonly reported difference in DAergic and non-DAergic neurons of the VTA is varying action potential half width. It is well documented that DAergic neurons

have a longer action potential duration, with the exact reason remaining unclear. The most likely explanation appears to be the fact that the axon in DAergic neurons usually emerges from a dendrite and not from the soma, as is the case for non-DAergic neurons. The distance between the soma and dendritic site, from which the axon emerges, can be as long as 240 μm (Häusser et al., 1995). Simultaneous somatic and dendritic recordings show that the action potentials always start in the axon and then spread through the axon-bearing dendrite to the soma. The long distance between the site of spike initiation and the soma may partially account for the slow rising phase of the action potential recorded from the DAergic cell soma (Häusser et al., 1995). In non-DAergic neurons, the axon usually emerges from a site near the soma and the action potential occurs first in the soma and then dendrites, accounting for the faster rising phase of the action potential (Häusser et al., 1995; Atherton & Bevan, 2005).

Overall, our results suggest no electrophysiological marker, on its own, can perfectly identify the neurotransmitter content of a VTA neuron. Even DA autoinhibition, while specific to DAergic cells, does not provide a ‘fool-proof’ method of identification. Although all DA cells tested in our work display a hyperpolarization, this hyperpolarization resulted in complete cessation of firing in only 60% of cells. In a circumstance where only the firing pattern is monitored, the remaining 40% of cells could appear to be DA insensitive.

4.3 LTCC modulation

Considering the manipulation of intrinsically expressed channels can have such a strong influence on firing patterns and frequency, as outlined in Chapter 1, and because increased internal calcium concentration can have such widespread effects on a cell, we wanted to investigate the role LTCCs play in firing pattern modulation of VTA neurons. As well, because the activity of GABAergic VTA neurons can play such an important role in the functioning of the reward pathway, we sought to investigate the regulation of both DAergic and non-DAergic neurons.

When LTCCs are open there are significant changes in the AHP profile of DAergic and non-DAergic cells. This may be due in large part to increased calcium concentrations activating SK channels, resulting in the observed decrease in mAHP. This, combined with the depolarization associated with the movement of calcium into the cell, extends depolarization, allowing multiple APs to be fired in quick succession (bursting).

4.3.1 FPL 64176 can induce burst firing in DAergic and non-DAergic neurons

Both cell populations (DAergic and non-DAergic) respond to 1 μ M FPL 64176 addition with similar depolarization, suggesting both cell populations express LTCC, and presumably have similar LTCC activity. This depolarization leads to a change in firing frequency and pattern in a selection of DAergic and non-DAergic cells.

Calcium influx through LTCCs further increases intracellular calcium levels through calcium-induced calcium release from internal stores. This triggers a cascade of

cellular events leading to LTCC modulation (Berridge, 1998). As well, increased intracellular calcium levels regulate calcium-activated K^+ channels, (Morikawa et al., 2000) which play a role in shaping firing patterns. Previous work from our lab has shown, however, that internal calcium stores are not necessary for LTCC mediated burst firing. LTCC mediated bursting can be induced and maintained even when internal calcium stores are depleted.

The opening of L-type calcium channels using FPL 64176 did not induce burst firing until about 25 min following the start of drug application and lasted for hours. The lag in burst firing development seems to indicate that calcium entry activated a signaling cascade that takes time to develop or a second messenger must migrate between the intracellular compartments. Previous work in our lab has identified that calcium entry through LTCCs activates the calcium-dependent protease calpain which cleaves PKC into PKM to induce burst firing in DAergic VTA neurons (Liu et al., 2007). Whether calcium entry through LTCCs activates the same signaling cascade in non-DAergic neurons remains unknown, however given that FPL 64176 induces bursting along a similar time course in both cell populations it is likely PKM is also mediating LTCC induced burst firing in GABAergic neurons.

Previous work in our lab has shown that putative DAergic neurons (electrophysiologically identified) burst fire in response to the LTCC opener FPL (approx 60% of cells). The portion of bursting DAergic neurons reported in this thesis is smaller, 36.4%. I feel that the decreased amount of induced bursting is due to two main factors: sample size and technical considerations. Although my groups are smaller than previous

studies, this does not account for all of the difference in proportion of cells responding to LTCC opener. Previous work used the blind patch method, allowing deeper cells to be targeted (essentially anywhere in a 300 μm thick slice), as opposed to a maximum depth of 100 μm in a 300 μm slice using a DIC mediated set up. DIC assisted patch forces more superficial cell layers to be targeted—cells which may not be quite as healthy as cells in deeper layers. During slice cutting superficial cell layers incur more abuse than cells in layers below. Similarly, these superficial cells are not held in place as tightly, so move (shrink or swell) substantially more than cells in the deeper layers. This, however, cannot fully explain the difference in behavior seen in my experiments. There is also the possibility that EGFP expressed in the cells is having an effect. Although clearly not detrimental to the cell, as all basic properties and firing patterns are similar to expected values, the presence of EGFP may be interfering with some protein interactions required for bursting. The entire signaling cascade required for burst firing is not fully understood, and it is possible, albeit unlikely, the EGFP is partially interfering with vital processes somewhere in the signaling cascade leading to bursting. Considering a mouse homozygous for EGFP dies at approximately postnatal day 21 due to EGFP build up, it must be questioned whether heterozygous EGFP mice are suffering minor EGFP induced deficits.

It should be noted that this thesis does not differentiate between the two GABAergic cell populations in the VTA; we examined the response of all GABAergic cells as one group. Initially the μ -opioid agonist DAMGO was used to differentiate GABAergic interneurons and GABAergic projection neurons, as interneurons are

inhibited by DAMGO (Johnson et al., 1992a; Johnson et al., 1992b; Cameron et al., 1997; Chieng et al., 2011). This experiment was ultimately abandoned due to time constraints. Sufficient access was commonly lost before a complete LTCC agonist/antagonist protocol, which was our highest priority, could be completed. As we were most interested in comparing basic electrophysiological properties and LTCC modulation between DAergic and non-DAergic neurons, differentiating between GABAergic interneurons and GABAergic projection cells became the lowest priority experiment.

4.3.2 AHP profile and LTCC mediated bursting

When grouped solely based on response to FPL 64176, the cells with a more depolarized baseline resting membrane potential were the same cells that went on to burst fire. Also, the cells that went on to burst fire had larger mAHPs during baseline conditions. A likely explanation for this observation is that these cells are expressing more LTCCs and have more intrinsically active LTCCs during baseline conditions. Unfortunately, this question was not fully answered during the course of my work, but would be an interesting future experiment. The cell groups are quite small, but bursting cells in the presence of nifedipine often converted to single spiking at a level below baseline, suggesting some LTCCs were intrinsically active. Future experiments looking at the change in firing activity in response to an LTCC antagonist during baseline may provide insight into this. Similarly, cells which went on to burst firing in response to LTCC activation showed a significant decrease in mAHP from baseline to bursting, significantly larger than the cells which did not respond with burst firing. mAHP allows or inhibits multiple APs to be fired in a row therefore a decrease in mAHP will allow

multiple APs to be fired in quick succession (bursting). In the case of non-bursting cells, the mAHP is not decreased enough to allow multiple APs to fire during a single depolarization. Due to the slow kinetics of sAHP, the sAHP of each AP within a burst will summate to give a large post burst hyperpolarization, resulting in a quiet period between bursting cycles. For this reason, a significant change in sAHP is observed in bursting neurons but not in non-bursting neurons in this study.

4.3.3 LTCC subtype involvement

There are four subtypes of LTCCs, although only Ca_v1.2 and Ca_v1.3 subtypes are expressed in VTA neurons (Chan, et al., 2007; Takada, et al., 2001). L-type calcium channels are often assumed to be active between -40 and -20 mV and therefore are considered high voltage-activated (Ertel, et al., 2000). While Ca_v1.2 LTCCs display this typical voltage dependency (Mori, et al., 1993), Ca_v1.3 LTCCs activate at relatively hyperpolarized membrane potentials (between -50 and -55 mV) and are incompletely inhibited by DHP antagonists (Xu and Lipscombe, 2001). The large difference in activation thresholds between these two subtypes suggest that they may be coupled to different molecular signaling pathways (Zhang, et al., 2006) so as to mediate different physiological roles in neuronal electrical tasks. For example, because Ca_v1.3 LTCCs activate near resting membrane potential, Ca_v1.3 channels are likely to be important in mediating calcium influx in response to relatively small membrane depolarization. Such properties may be important for sustaining spontaneous rhythmic firing in neurons, traditionally attributed to the activities of low-threshold T-type calcium channels (Bean, 1989; Ertel, et al., 2000). Different from rhythmic firing, burst firing is a combination of

subthreshold depolarization and clustered action potential firing. It is likely the underlying subthreshold depolarization is mediated by Ca_v1.3, which is activated at relatively hyperpolarized membrane potentials (Xu and Lipscombe, 2001) and Ca_v1.2, which is high-voltage activated, is involved in the clustered fast firing (Mori, et al., 1993). It is reasonable to presume that Ca_v1.3 LTCCs mediate the subthreshold depolarization that raises the membrane potential to activate sodium channels initiating firing and then Ca_v1.2 L-type calcium channels take over to maintain sequential firing. However, my results support the hypothesis that only Ca_v1.3 LTCCs are involved in bursting. Activating both Ca_v1.2 and Ca_v1.3 subtypes by FPL 64176 induced burst firing similar to bursting induced by activating Ca_v1.3 alone ((S)-(-)-Bay K8644 in Ca_v1.2DHP^{+/+} slices). Similarly, bursting induced by activating both subtypes with FPL 64176 could be blocked with nifedipine (which blocks Ca_v1.2 and Ca_v1.3 in wild type slices and Ca_v1.3 only in Ca_v1.2DHP^{+/+} slices). Taken together these results suggest Ca_v1.3 LTCCs are required for burst firing while Ca_v1.2 LTCCs are not necessary for bursting, although they may participate in maintaining bursting in some way. Unpublished work from our lab using a Ca_v1.3 knock-out mouse model has demonstrated that in the absence of Ca_v1.3 channels, activating Ca_v1.2 channels will result in burst firing. Taken together this data suggests Ca_v1.3 has a stronger impact on firing pattern modulation than Ca_v1.2, however in the absence of Ca_v1.3, the Ca_v1.2 channels will take over this role.

Consistent with previous reports from our lab using electrophysiologically identified DAergic cells, the Ca_v1.3 subtype underlies firing pattern modulation in DAergic cells, but novel to this study, it also is the LTCC subtype underlying firing

pattern modulation in non-DAergic cells. At first it seems odd to have the same channel modulating activity of two cell populations with opposite functional outputs. GABAergic interneurons inhibit DAergic cells in the VTA, yet LTCC activation excites both cell populations. It is possible the LTCCs of GABAergic and DAergic cells are not active on the same time course. For example, it is possible that when GABAergic cells are bursting DAergic cells are quiet, then when GABAergic cells are quiet DAergic cells burst fire. Or maybe the DAergic and GABAergic projection neurons are bursting together, but the interneurons are not responding with bursting. As previously discussed, this thesis does not differentiate between GABAergic interneurons and GABAergic projection neurons, so cannot answer these questions. Future experiments to address these issues will be discussed later. Our work also identified a substantial population of both DAergic and GABAergic neurons that did not burst fire in response to LTCC modulation. The difference in this cell population and the bursting cells remains unclear, but the observation of this cell population having a more hyperpolarized resting membrane potential during baseline and less change in mAHP in response to an LTCC agonist suggests there is a difference in channel expression.

4.4 Conclusions

Understanding the intrinsic modulators of firing pattern regulation in both DAergic and non-DAergic neurons of the VTA can provide a better understanding of disease states associated with dysregulation in this area, potentially leading to a target for future treatment options. This thesis not only implicates the Ca_v1.3 LTCC in firing

pattern modulation of DAergic and non-DAergic neurons of the VTA, but also demonstrates the EGFP labeled TH⁺-cell mouse model as a reliable method of cell identification. LTCC induced bursting can provide an *in vitro* model of burst firing, serving as an electrophysiological testing platform to examine cellular signaling pathways that underlie behaviours such as addiction, while the EGFP expressing animal model can differentiate the DAergic and GABAergic population. Taken together, these two models can greatly aid in increasing our understanding of both VTA cell populations.

As previously discussed, Ca_v1.3 LTCCs are one of the four subtypes of LTCCs, but due to technical difficulties in pharmacologically isolating Ca_v1.3 from Ca_v1.2 LTCCs, the specific functional roles of each channel subtype have long remained obscure. The recent development of transgenic animals has led to Ca_v1.3 LTCCs being implicated in addiction and other diseases. For example, Ca_v1.3-deficient mice lack amphetamine-sensitized locomotor activity (Giordano, et al., 2006) and exhibit an antidepressant-like phenotype (Striessnig, et al., 2006). In addition, the expression of Cav1.3 LTCCs is decreased by chronic morphine treatment in midbrain regions of mice (Haller, et al., 2008). More importantly, Ca_v1.3 LTCCs can mediate all of these behaviours by their role in regulating firing patterns reported in my thesis because burst firing elevates terminal field DA levels more efficiently and all of these behaviours arise from increased DA transmission. Ca_v1.3 LTCCs might play a significant role in central DA transmission and its related pathologies such as drug abuse.

4.5 Future Directions

Future research directed from my thesis should focus on three main points: determining the LTCC subtype expression and activity within and between VTA neuronal populations; investigating whether Ca_v1.2 is upregulated when Ca_v1.3 is knocked out; and determine whether GABA projection neurons function the same as GABA interneurons.

Firstly, using immunohistochemistry and the TH-EGFP mouse model, the number and expression pattern of both LTCC subtypes could be evaluated for DAergic and GABAergic cells in the VTA. It is likely a subpopulation of both DAergic and GABAergic cells, corresponding to the non-bursting cells, are expressing fewer LTCCs than the cells that respond to LTCC agonist with burst firing. As well, bursting and non-bursting cells may be expressing the LTCC subtypes in different ratios (Ca_v1.3: Ca_v1.2) and patterns, all of which will influence firing activity. Similarly, using electrophysiology the intrinsic activity of LTCCs can be measured during baseline conditions. The intrinsic activity of LTCCs may be a predictor of whether the cell will respond to LTCC agonist with burst firing.

Secondly, using a Ca_v1.3 knock out mouse model, our lab observed Ca_v1.2 mediates burst firing in DAergic neurons in the absence of Ca_v1.3 LTCCs (unpublished data). It would be of great interest to further investigate the compensatory role Cav1.2 takes on when Cav1.3 channels are non-functional. Of particular interest would be investigating whether the Cav1.2 channel is upregulated when Cav1.3 is knocked out.

Lastly, if these experiments were to be repeated I would like to have a reliable method of differentiating GABA interneurons and GABA projection neurons. Much of the data of this thesis pertaining to GABAergic cells is confounded by the fact that projection and interneurons have very different physiological functions so may have very different properties. In an effort to combat this issue it would be interesting to combine our current EGFP-TH mouse model with a mouse model containing interneurons expressing a different fluorescent protein. This would produce DAergic cells which fluoresce green, GABA interneurons which fluoresce a different color, and GABA projection neurons which do not fluoresce under any conditions. This would allow us to accurately determine whether GABAergic interneurons and projection neurons differ in basic electrophysiological properties as well as firing pattern modulation.

Reference List

- Akaoka, H., Charlety, P., Saunier, C. F., Buda, M., & Chouvet, G. (1992). Inhibition of nigral dopamine neurons by systemic and local apomorphine: possible contribution of dendritic autoreceptors. *Neuroscience*, *49*, 879-891.
- Albert, P. R., Neve, K. A., Bunzow, J. R., & Civelli, O. (1990). Coupling of a cloned rat dopamine-D2 receptor to inhibition of adenylyl cyclase and prolactin secretion. *Journal of Biological Chemistry*, *265*, 2098-2104.
- Alger, B. E. & Williamson, A. (1988). A transient calcium-dependent potassium component of the epileptiform burst after-hyperpolarization in rat hippocampus. *Journal of Physiology-London*, *399*, 191-205.
- Amara, S. G. & Kuhar, M. J. (1993). Neurotransmitter transporters: recent progress. *Annual Review of Neuroscience*, *16*, 73-93.
- Andersen, P. H., Gingrich, J. A., Bates, M. D., Dearry, A., Falardeau, P., Senogles, S. E. et al. (1990). Dopamine receptor subtypes - beyond the D1/d2 classification. *Trends in pharmacological sciences*, *11*, 231-236.
- Atherton, J. F. & Bevan, M. D. (2005). Ionic mechanisms underlying autonomous action potential generation in the somata and dendrites of GABAergic substantia nigra pars reticulata neurons in vitro. *Journal of Neuroscience*, *25*, 8272-8281.

Balfour, D. J., Wright, A. E., Benwell, M. E., & Birrell, C. E. (2000). The putative role of extra-synaptic mesolimbic dopamine in the neurobiology of nicotine dependence. *Behavioural brain research*, *113*, 73-83.

Barnard, E. A., Skolnick, P., Olsen, R. W., Mohler, H., Sieghart, W., Biggio, G. et al. (1998). International Union of Pharmacology. XV. Subtypes of gamma-aminobutyric acid(A) receptors: Classification on the basis of subunit structure and receptor function. *Pharmacological Reviews*, *50*, 291-313.

Beart, P. M. & McDonald, D. (1980). Neurochemical studies of the mesolimbic dopaminergic pathway - somatodendritic mechanisms and gabaergic neurons in the rat ventral tegmentum. *Journal of neurochemistry*, *34*, 1622-1629.

Beart, P. M., McDonald, D., & Gundlach, A. L. (1979). Mesolimbic dopaminergic neurones and somatodendritic mechanisms. *Neuroscience letters*, *15*, 165-170.

Bentivoglio, M. & Morelli, M. (2005). The organization and circuits of mesencephalic dopaminergic neurons and the distribution of dopamine receptors in the brain. In S.B.Dunnett (Ed.), *Handbook of Chemical Neuroanatomy Dopamine* (Volume 21 ed., pp. 1-107). Elsevier.

Berke, J. D. & Hyman, S. E. (2000). Addiction, dopamine, and the molecular mechanisms of memory. *Neuron*, *25*, 515-532.

Berridge, M. J. (1998). Neuronal calcium signaling. *Neuron*, *21*, 13-26.

Bjorklund, A. & Dunnett, S. B. (2007). Dopamine neuron systems in the brain: an update. *Trends in neurosciences*, 30, 194-202.

Blythe, S. N., Atherton, J. F., & Bevan, M. D. (2007). Synaptic activation of dendritic AMPA and NMDA receptors generates transient high-frequency firing in substantia nigra dopamine neurons in vitro. *Journal of neurophysiology*, 97, 2837-2850.

Bond, C. T., Herson, P. S., Strassmaier, T., Hammond, R., Stackman, R., Maylie, J. et al. (2004). Small conductance Ca²⁺-activated K⁺ channel knock-out mice reveal the identity of calcium-dependent afterhyperpolarization currents. *Journal of Neuroscience*, 24, 5301-5306.

Bouthenet, M. L., Martres, M. P., Sales, N., & Schwartz, J. C. (1987). A detailed mapping of dopamine D-2 Receptors in rat central-nervous-system by autoradiography with [I-125] iodospripide. *Neuroscience*, 20, 117-155.

Bradberry, C. W. & Roth, R. H. (1989). Cocaine increases extracellular dopamine in rat nucleus accumbens and ventral tegmental area as shown by in vivo microdialysis. *Neuroscience letters*, 103, 97-102.

Braszko, J. J., Bannon, M. J., Bunney, B. S., & Roth, R. H. (1981). Intraatrial kainic acid: acute effects on electrophysiological and biochemical measures of nigrostriatal dopaminergic activity. *The Journal of pharmacology and experimental therapeutics*, 216, 289-293.

Brodie, M. S., Scholz, A., Weiger, T. M., & Dopico, A. M. (2007). Ethanol interactions with calcium-dependent potassium channels. *Alcoholism-Clinical and Experimental Research*, *31*, 1625-1632.

Calabresi, P., Lacey, M. G., & North, R. A. (1989). Nicotinic excitation of rat ventral tegmental neurones in vitro studied by intracellular recording. *British journal of pharmacology*, *98*, 135-140.

Cameron, D. L., Wessendorf, M. W., & Williams, J. T. (1997). A subset of ventral tegmental area neurons is inhibited by dopamine, 5-hydroxytryptamine and opioids. *Neuroscience*, *77*, 155-166.

Cardozo, D. L. & Bean, B. P. (1995). Voltage-dependent calcium channels in rat midbrain dopamine neurons - modulation by dopamine and Gaba(B) receptors. *Journal of neurophysiology*, *74*, 1137-1148.

Carlsson, A. (1988). The current status of the dopamine hypothesis of schizophrenia. *Neuropsychopharmacology : official publication of the American College of Neuropsychopharmacology*, *1*, 179-186.

Carlsson, A., Lindquest, M., Magnusson, T., & Waldeck, B. (1958). On the presence of 3-hydroxytyramine in brain. *Science (New York, N.Y.)*, *127*, 471.

Carr, D. B. & Sesack, S. R. (2000). Projections from the rat prefrontal cortex to the ventral tegmental area: target specificity in the synaptic associations with

mesoaccumbens and mesocortical neurons. *The Journal of neuroscience : the official journal of the Society for Neuroscience*, 20, 3864-3873.

Catania, M. V., De Socarraz, H., Penney, J. B., & Young, A. B. (1994). Metabotropic glutamate receptor heterogeneity in rat brain. *Molecular pharmacology*, 45, 626-636.

Caulfield, M. P. (1993). Muscarinic receptors--characterization, coupling and function. *Pharmacology & therapeutics*, 58, 319-379.

Chan, C. S., Guzman, J. N., Ilijic, E., Mercer, J. N., Rick, C., Tkatch, T. et al. (2007). 'Rejuvenation' protects neurons in mouse models of Parkinson's disease. *Nature*, 447, 1081-1086.

Changizi, M. A., McGehee, R. M. F., & Hall, W. G. (2002). Evidence that appetitive responses for dehydration and food-deprivation are learned. *Physiology & Behavior*, 75, 295-304.

Chen, J. F., Qin, Z. H., Szele, F., Bai, G., & Weiss, B. (1991). Neuronal localization and modulation of the D2 dopamine receptor messenger-RNA in brain of normal mice and mice lesioned with 6-Hydroxydopamine. *Neuropharmacology*, 30, 927- &.

Chen, Y., Phillips, K., Minton, G., & Sher, E. (2005). GABA(B) receptor modulators potentiate baclofen-induced depression of dopamine neuron activity in the rat ventral tegmental area. *British journal of pharmacology*, 144, 926-932.

Cheramy, A., Leviel, V., & Glowinski, J. (1981). Dendritic release of dopamine in the substantia nigra. *Nature*, 289, 537-542.

Chieng, B., Azriel, Y., Mohammadi, S., & Christie, M. J. (2011). Distinct cellular properties of identified dopaminergic and GABAergic neurons in the mouse ventral tegmental area. *Journal of Physiology-London*, 589, 3775-3787.

Christoffersen, C. L. & Meltzer, L. T. (1995). Evidence for N-methyl-D-aspartate and AMPA subtypes of the glutamate receptor on substantia nigra dopamine neurons: possible preferential role for N-methyl-D-aspartate receptors. *Neuroscience*, 67, 373-381.

Churchill, L., Dilts, R. P., & Kalivas, P. W. (1992). Autoradiographic localization of Gamma-Aminobutyric Acida receptors within the ventral tegmental area. *Neurochemical Research*, 17, 101-106.

Clark, D. & Chiodo, L. A. (1988). Electrophysiological and pharmacological characterization of identified nigrostriatal and mesoaccumbens dopamine neurons in the rat. *Synapse (New York, N.Y.)*, 2, 474-485.

Clarke, P. B. & Pert, A. (1985). Autoradiographic evidence for nicotine receptors on nigrostriatal and mesolimbic dopaminergic neurons. *Brain research*, 348, 355-358.

Clarke, P. B., Schwartz, R. D., Paul, S. M., Pert, C. B., & Pert, A. (1985). Nicotinic binding in rat brain: autoradiographic comparison of [3H]acetylcholine, [3H]nicotine, and [125I]-alpha-bungarotoxin. *The Journal of neuroscience : the official journal of the Society for Neuroscience*, 5, 1307-1315.

Corrigall, W. A., Coen, K. M., & Adamson, K. L. (1994). Self-administered nicotine activates the mesolimbic dopamine system through the ventral tegmental area. *Brain research*, 653, 278-284.

Cox, R. H., Folander, K., & Swanson, R. (1998). Voltage-gated potassium channel expression in rat arterial smooth muscle. *Biophysical Journal*, 74, A112.

Dani, J. A. & De Biasi, M. (2001). Cellular mechanisms of nicotine addiction. *Pharmacology, biochemistry, and behavior*, 70, 439-446.

Dawson, T. M., Gehlert, D. R., Yamamura, H. I., Bernett, A., & Wamsley, J. K. (1985). D-1 Dopamine-Receptors in the Rat-Brain - Autoradiographic Localization using [H-3]sch 23390. *European journal of pharmacology*, 108, 323-325.

Dearry, A., Gingrich, J. A., Falardeau, P., Freneau, R. T., Bates, M. D., & Caron, M. G. (1990). Molecular-Cloning and Expression of the Gene for a Human D1 Dopamine Receptor. *Nature*, 347, 72-76.

DeLong, M. R. (1990). Primate Models of Movement-Disorders of Basal Ganglia Origin. *Trends in neurosciences*, 13, 281-285.

Di Chiara, G. (1995). The role of dopamine in drug abuse viewed from the perspective of its role in motivation. *Drug and alcohol dependence*, 38, 95-137.

Di Chiara, G. (1999). Drug addiction as dopamine-dependent associative learning disorder. *European journal of pharmacology*, 375, 13-30.

Di Chiara, G. & Imperato, A. (1988). Drugs abused by humans preferentially increase synaptic dopamine concentrations in the mesolimbic system of freely moving rats. *Proceedings of the National Academy of Sciences of the United States of America*, *85*, 5274-5278.

Druhan, J. P., Fibiger, H. C., & Phillips, A. G. (1989). Differential effects of cholinergic drugs on discriminative cues and self-stimulation produced by electrical stimulation of the ventral tegmental area. *Psychopharmacology*, *97*, 331-338.

Durante, P., Cardenas, C. G., Whittaker, J. A., Kitai, S. T., & Scroggs, R. S. (2004). Low-threshold L-type calcium channels in rat dopamine neurons. *Journal of neurophysiology*, *91*, 1450-1454.

Einhorn, L. C., Johansen, P. A., & White, F. J. (1988). Electrophysiological effects of cocaine in the mesoaccumbens dopamine system: studies in the ventral tegmental area. *The Journal of neuroscience : the official journal of the Society for Neuroscience*, *8*, 100-112.

Engberg, G., Kling-Petersen, T., & Nissbrandt, H. (1993). GABAB-receptor activation alters the firing pattern of dopamine neurons in the rat substantia nigra. *Synapse (New York, N.Y.)*, *15*, 229-238.

Erhardt, S., Andersson, B., Nissbrandt, H., & Engberg, G. (1998). Inhibition of firing rate and changes in the firing pattern of nigral dopamine neurons by gamma-

hydroxybutyric acid (GHBA) are specifically induced by activation of GABA(B) receptors. *Naunyn-Schmiedeberg's archives of pharmacology*, 357, 611-619.

Erhardt, S. & Engberg, G. (2000). Excitation of nigral dopamine neurons by the GABA(A) receptor agonist muscimol is mediated via release of glutamate. *Life Sciences*, 67, 1901-1911.

Erhardt, S., Mathe, J. M., Chergui, K., Engberg, G., & Svensson, T. H. (2002). GABA(B) receptor-mediated modulation of the firing pattern of ventral tegmental area dopamine neurons in vivo. *Naunyn-Schmiedeberg's archives of pharmacology*, 365, 173-180.

Fallon, J. H. (1981). Collateralization of monoamine neurons - mesotelencephalic dopamine projections to caudate, septum, and frontal-cortex. *Journal of Neuroscience*, 1, 1361-1368.

Fallon, J. H. & Moore, R. Y. (1978). Catecholamine innervation of basal forebrain .4. Topography of dopamine projection to basal forebrain and neostriatum. *Journal of Comparative Neurology*, 180, 545-&.

Fiorillo, C. D. & Williams, J. T. (1998). Glutamate mediates an inhibitory postsynaptic potential in dopamine neurons. *Nature*, 394, 78-82.

Floresco, S. B., Todd, C. L., & Grace, A. A. (2001). Glutamatergic afferents from the hippocampus to the nucleus accumbens regulate activity of ventral tegmental area

dopamine neurons. *The Journal of neuroscience : the official journal of the Society for Neuroscience*, 21, 4915-4922.

Floresco, S. B., West, A. R., Ash, B., Moore, H., & Grace, A. A. (2003). Afferent modulation of dopamine neuron firing differentially regulates tonic and phasic dopamine transmission. *Nature neuroscience*, 6, 968-973.

Forster, G. L., Falcon, A. J., Miller, A. D., Heruc, G. A., & Blaha, C. D. (2002). Effects of laterodorsal tegmentum excitotoxic lesions on behavioral and dopamine responses evoked by morphine and d-amphetamine. *Neuroscience*, 114, 817-823.

Freeman, A. S. & Bunney, B. S. (1987). Activity of A9 and A10 dopaminergic neurons in unrestrained rats: further characterization and effects of apomorphine and cholecystokinin. *Brain research*, 405, 46-55.

Fu, L. Y., Wang, F., Chen, X. S., Zhou, H. Y., Yao, W. X., Xia, G. J. et al. (2003). Perforated patch recording of L-type calcium current with beta-escin in guinea pig ventricular myocytes. *Acta Pharmacologica Sinica*, 24, 1094-1098.

Gahn, L. G. & Roskoski, R. (1995). Thermal-stability and Cd analysis of rat tyrosine-hydroxylase. *Biochemistry*, 34, 252-256.

Gariano, R. F. & Groves, P. M. (1988). Burst firing induced in midbrain dopamine neurons by stimulation of the medial prefrontal and anterior cingulate cortices. *Brain research*, 462, 194-198.

Gariano, R. F., Sawyer, S. F., Tepper, J. M., Young, S. J., & Groves, P. M. (1989). Mesocortical dopaminergic neurons. 2. Electrophysiological consequences of terminal autoreceptor activation. *Brain research bulletin*, 22, 517-523.

Goto, Y. & Grace, A. A. (2007). The dopamine system and the pathophysiology of schizophrenia: A basic science perspective. *Integrating the Neurobiology of Schizophrenia*, 78, 41-68.

Grace, A. A. & Bunney, B. S. (1979). Paradoxical GABA excitation of nigral dopaminergic cells: indirect mediation through reticulata inhibitory neurons. *European journal of pharmacology*, 59, 211-218.

Grace, A. A. & Bunney, B. S. (1983). Intracellular and extracellular electrophysiology of nigral dopaminergic-neurons .1. Identification and characterization. *Neuroscience*, 10, 301-315.

Grace, A. A. & Bunney, B. S. (1984). The control of firing pattern in nigral dopamine neurons: burst firing. *The Journal of neuroscience : the official journal of the Society for Neuroscience*, 4, 2877-2890.

Grace, A. A. & Bunney, B. S. (1995). Electrophysiological properties of midbrain dopamine neurons. In F.E.Bloom & D. J. Kupfer (Eds.), *Psychopharmacology: The Fourth Generation of Progress* (pp. 163-178). New York: Raven Press, Ltd.

Grace, A. A. & Onn, S. P. (1989). Morphology and electrophysiological properties of immunocytochemically identified rat dopamine neurons recorded invitro. *Journal of Neuroscience*, *9*, 3463-3481.

Grenhoff, J., Aston-Jones, G., & Svensson, T. H. (1986). Nicotinic effects on the firing pattern of midbrain dopamine neurons. *Acta Physiologica Scandinavica*, *128*, 351-358.

Grillner, P., Bonci, A., Svensson, T. H., Bernardi, G., & Mercuri, N. B. (1999). Presynaptic muscarinic (M3) receptors reduce excitatory transmission in dopamine neurons of the rat mesencephalon. *Neuroscience*, *91*, 557-565.

Hansen, H. H., Ebbesen, C., Mathiesen, C., Weikop, P., Ronn, L. C., Waroux, O. et al. (2006). The KCNQ channel opener retigabine inhibits the activity of mesencephalic dopaminergic systems of the rat. *Journal of Pharmacology and Experimental Therapeutics*, *318*, 1006-1019.

Häusser, M., Stuart, G., Racca, C., & Sakmann, B. (1995). Axonal initiation and active dendritic propagation of action-potentials in substantia-nigra neurons. *Neuron*, *15*, 637-647.

Hell, J. W., Westenbroek, R. E., Warner, C., Ahljianian, M. K., Prystay, W., Gilbert, M. M. et al. (1993). Identification and differential subcellular localization of the neuronal class C and class D L-type calcium channel alpha 1 subunits. *The Journal of cell biology*, *123*, 949-962.

Herrero, I., Miras-Portugal, M. T., & Sanchez-Prieto, J. (1992). Positive feedback of glutamate exocytosis by metabotropic presynaptic receptor stimulation. *Nature*, *360*, 163-166.

Hokfelt, T., Skirboll, L., Rehfeld, J. F., Goldstein, M., Markey, K., & Dann, O. (1980). A Sub-Population of Mesencephalic Dopamine Neurons Projecting to Limbic Areas Contains a Cholecystokinin-Like Peptide - Evidence from Immunohistochemistry Combined with Retrograde Tracing. *Neuroscience*, *5*, 2093-2124.

Howes, O. D. & Kapur, S. (2009). The dopamine hypothesis of schizophrenia: version III--the final common pathway. *Schizophrenia bulletin*, *35*, 549-562.

Hulme, E. C., Birdsall, N. J., & Buckley, N. J. (1990). Muscarinic receptor subtypes. *Annual Review of Pharmacology and Toxicology*, *30*, 633-673.

Huneke, R., Zitzelsberger, D., Fassl, J., Jungling, E., Brose, S., Buhre, W. et al. (2004). Temperature-independent inhibition of L-type calcium currents by halothane and sevoflurane in human atrial cardiomyocytes. *Anesthesiology*, *101*, 409-416.

Ikemoto, S., Kohl, R. R., & McBride, W. J. (1997). GABA(A) receptor blockade in the anterior ventral tegmental area increases extracellular levels of dopamine in the nucleus accumbens of rats. *Journal of neurochemistry*, *69*, 137-143.

Imperato, A., Mulas, A., & Di Chiara, G. (1986). Nicotine preferentially stimulates dopamine release in the limbic system of freely moving rats. *European journal of pharmacology*, *132*, 337-338.

Innis, R. B. & Aghajanian, G. K. (1987). Pertussis toxin blocks autoreceptor-mediated inhibition of dopaminergic neurons in rat substantia nigra. *Brain research*, 411, 139-143.

Johnson, S. W. & North, R. A. (1992a). Opioids excite dopamine neurons by hyperpolarization of local interneurons. *Journal of Neuroscience*, 12, 483-488.

Johnson, S. W. & North, R. A. (1992b). Two types of neurone in the rat ventral tegmental area and their synaptic inputs. *The Journal of physiology*, 450, 455-468.

Johnson, S. W. & Seutin, V. (1997). Bicuculline methiodide potentiates NMDA-dependent burst firing in rat dopamine neurons by blocking apamin-sensitive Ca²⁺-activated K⁺ currents. *Neuroscience letters*, 231, 13-16.

Johnson, S. W., Seutin, V., & North, R. A. (1992c). Burst firing in dopamine neurons induced by N-methyl-D-aspartate: role of electrogenic sodium pump. *Science (New York, N.Y.)*, 258, 665-667.

Johnson, S. W. & Wu, Y. N. (2004). Multiple mechanisms underlie burst firing in rat midbrain dopamine neurons in vitro. *Brain research*, 1019, 293-296.

Kalivas, P. W. & Duffy, P. (1991). A comparison of axonal and somatodendritic dopamine release using in vivo dialysis. *Journal of neurochemistry*, 56, 961-967.

- Kaneko, T., Akiyama, H., Nagatsu, I., & Mizuno, N. (1990). Immunohistochemical demonstration of glutaminase in catecholaminergic and serotonergic neurons of rat-brain. *Brain research*, *507*, 151-154.
- Kim, S. H., Choi, Y. M., Chung, S., Uhm, D. Y., & Park, M. K. (2004). Two different Ca²⁺-dependent inhibitory mechanisms of spontaneous firing by glutamate in dopamine neurons. *Journal of neurochemistry*, *91*, 983-995.
- Kitai, S. T., Shepard, P. D., Callaway, J. C., & Scroggs, R. (1999). Afferent modulation of dopamine neuron firing patterns. *Current opinion in neurobiology*, *9*, 690-697.
- Koob, G. F. (1992). Drugs of abuse - anatomy, pharmacology and function of reward pathways. *Trends in pharmacological sciences*, *13*, 177-184.
- Koob, G. F. (1996). Drug addiction: The Yin and Yang of hedonic homeostasis. *Neuron*, *16*, 893-896.
- Koob, G. F., Sanna, P. P., & Bloom, F. E. (1998). Neuroscience of addiction. *Neuron*, *21*, 467-476.
- Koyama, S. & Appel, S. B. (2006). Characterization of M-current in ventral tegmental area dopamine neurons. *Journal of neurophysiology*, *96*, 535-543.

Lacey, M. G., Calabresi, P., & North, R. A. (1990). Muscarine depolarizes rat substantia nigra zona compacta and ventral tegmental neurons in vitro through M1-like receptors. *The Journal of pharmacology and experimental therapeutics*, 253, 395-400.

Lacey, M. G., Mercuri, N. B., & North, R. A. (1987). Dopamine acts on D2 receptors to increase potassium conductance in neurones of the rat substantia nigra zona compacta. *The Journal of physiology*, 392, 397-416.

Lammel, S., Hetzel, A., Hackel, O., Jones, I., Liss, B., & Roeper, J. (2008). Unique properties of mesoprefrontal neurons within a dual mesocorticolimbic dopamine system. *Neuron*, 57, 760-773.

Lassen, M. B., Brown, J. E., Stobbs, S. H., Gunderson, S. H., Maes, L., Valenzuela, C. F. et al. (2007). Brain stimulation reward is integrated by a network of electrically coupled GABA neurons. *Brain research*, 1156, 46-58.

Laviolette, S. R. (2007). Dopamine modulation of emotional processing in cortical and subcortical neural circuits: Evidence for a final common pathway in schizophrenia? *Schizophrenia bulletin*, 33, 971-981.

Le Moal, M. & Simon, H. (1991). Mesocorticolimbic dopaminergic network - functional and regulatory roles. *Physiological reviews*, 71, 155-234.

Lipscombe, D., Helton, T. D., & Xu, W. (2004). L-type calcium channels: the low down. *Journal of neurophysiology*, 92, 2633-2641.

Lisman, J. E. & Grace, A. A. (2005). The hippocampal-VTA loop: Controlling the entry of information into long-term memory. *Neuron*, *46*, 703-713.

Liu, L., Xu, W., Harrington, K. A., & Emson, P. C. (1994). The molecular cloning and expression of a human synaptic vesicle amine transporter that suppresses MPP+ toxicity. *Brain research.Molecular brain research*, *25*, 90-96.

Liu, Y. & Chen, X. (2008). Cholinergic excitation of dopaminergic cells depends on sequential activation of protein kinase C and the L-type calcium channel in ventral tegmental area slices. *Brain research*, *1245*, 41-51.

Liu, Y., Dore, J., & Chen, X. (2007). Calcium influx through L-type channels generates protein kinase M to induce burst firing of dopamine cells in the rat ventral tegmental area. *The Journal of biological chemistry*, *282*, 8594-8603.

Lodge, D. J. & Grace, A. A. (2006). The laterodorsal tegmentum is essential for burst firing of ventral tegmental area dopamine neurons. *Proceedings of the National Academy of Sciences of the United States of America*, *103*, 5167-5172.

Lokwan, S. J., Overton, P. G., Berry, M. S., & Clark, D. (1999). Stimulation of the pedunculopontine tegmental nucleus in the rat produces burst firing in A9 dopaminergic neurons. *Neuroscience*, *92*, 245-254.

Louis, M. & Clarke, P. B. (1998). Effect of ventral tegmental 6-hydroxydopamine lesions on the locomotor stimulant action of nicotine in rats. *Neuropharmacology*, *37*, 1503-1513.

Mansvelter, H. D. & McGehee, D. S. (2000). Long-term potentiation of excitatory inputs to brain reward areas by nicotine. *Neuron*, 27, 349-357.

Margolis, E. B., Lock, H., Hjelmstad, G. O., & Fields, H. L. (2006). The ventral tegmental area revisited: is there an electrophysiological marker for dopaminergic neurons? *The Journal of physiology*, 577, 907-924.

Marinelli, M. & White, F. J. (2000). Enhanced vulnerability to cocaine self-administration is associated with elevated impulse activity of midbrain dopamine neurons. *The Journal of neuroscience : the official journal of the Society for Neuroscience*, 20, 8876-8885.

Matsushita, N., Okada, H., Yasoshima, Y., Takahashi, K., Kiuchi, K., & Kobayashi, K. (2002). Dynamics of tyrosine hydroxylase promoter activity during midbrain dopaminergic neuron development. *Journal of neurochemistry*, 82, 295-304.

McLean, J. H. & Shipley, M. T. (1988). Postmitotic, postmigrational expression of tyrosine-hydroxylase in olfactory-bulb dopaminergic-neurons. *Journal of Neuroscience*, 8, 3658-3669.

Meltzer, L. T., Christoffersen, C. L., & Serpa, K. A. (1997). Modulation of dopamine neuronal activity by glutamate receptor subtypes. *Neuroscience and biobehavioral reviews*, 21, 511-518.

Mercuri, N. B., Bonci, A., Calabresi, P., Stratta, F., Stefani, A., & Bernardi, G. (1994). Effects of dihydropyridine calcium-antagonists on rat midbrain dopaminergic-neurons. *British journal of pharmacology*, *113*, 831-838.

Mercuri, N. B., Calabresi, P., & Bernardi, G. (1992a). The electrophysiological actions of dopamine and dopaminergic drugs on neurons of the substantia nigra pars compacta and ventral tegmental area. *Life Sciences*, *51*, 711-718.

Mercuri, N. B., Stratta, F., Calabresi, P., & Bernardi, G. (1992b). Electrophysiological evidence for the presence of ionotropic and metabotropic excitatory amino acid receptors on dopaminergic neurons of the rat mesencephalon: an in vitro study. *Functional neurology*, *7*, 231-234.

Mercuri, N. B., Stratta, F., Calabresi, P., Bonci, A., & Bernardi, G. (1993). Activation of metabotropic glutamate receptors induces an inward current in rat dopamine mesencephalic neurons. *Neuroscience*, *56*, 399-407.

Mereu, G., Lilliu, V., Casula, A., Vargiu, P. F., Diana, M., Musa, A. et al. (1997). Spontaneous bursting activity of dopaminergic neurons in midbrain slices from immature rats: Role of N-methyl-D-aspartate receptors. *Neuroscience*, *77*, 1029-1036.

Missale, C., Nash, S. R., Robinson, S. W., Jaber, M., & Caron, M. G. (1998). Dopamine receptors: from structure to function. *Physiological reviews*, *78*, 189-225.

Monsma, F. J., Mahan, L. C., MCVITTIE, L. D., Gerfen, C. R., & Sibley, D. R. (1990). Molecular-cloning and expression of a d1 dopamine receptor linked to adenylyl

cyclase activation. *Proceedings of the National Academy of Sciences of the United States of America*, 87, 6723-6727.

Moore, R. Y. & Bloom, F. E. (1978). Central catecholamine neuron systems - anatomy and physiology of the dopamine systems. *Annual Review of Neuroscience*, 1, 129-169.

Morikawa, H., Imani, F., Khodakhah, K., & Williams, J. T. (2000). Inositol 1,4,5-triphosphate-evoked responses in midbrain dopamine neurons. *Journal of Neuroscience*, 20, art-RC103.

Morikawa, H., Khodakhah, K., & Williams, J. T. (2003). Two intracellular pathways mediate metabotropic glutamate receptor-induced Ca²⁺ mobilization in dopamine neurons. *The Journal of neuroscience : the official journal of the Society for Neuroscience*, 23, 149-157.

Nair-Roberts, R. G., Chatelain-Badie, S. D., Benson, E., White-Cooper, H., Bolam, J. P., & Ungless, M. A. (2008). Stereological estimates of dopaminergic, GABAergic and glutamatergic neurons in the ventral tegmental area, substantia nigra and retrorubral field in the rat. *Neuroscience*, 152, 1024-1031.

Nakajo, K. & Kubo, Y. (2005). Protein kinase C shifts the voltage dependence of KCNQ/M channels expressed in *Xenopus* oocytes. *Journal of Physiology-London*, 569, 59-74.

Nastuk, M. A. & Graybiel, A. M. (1991). Pharmacologically defined M1 and M2 muscarinic cholinergic binding sites in the cat's substantia nigra: development and maturity. *Brain research. Developmental brain research*, 61, 1-10.

Neuhoff, H., Neu, A., Liss, B., & Roeper, J. (2002). I-h channels contribute to the different functional properties of identified dopaminergic subpopulations in the midbrain. *Journal of Neuroscience*, 22, 1290-1302.

Neve, K. A., Cox, B. A., Henningsen, R. A., Spanoyannis, A., & Neve, R. L. (1991). Pivotal role for aspartate-80 in the regulation of dopamine-D2 receptor affinity for drugs and inhibition of adenylyl cyclase. *Molecular pharmacology*, 39, 733-739.

Nisell, M., Nomikos, G. G., & Svensson, T. H. (1994). Infusion of nicotine in the ventral tegmental area or the nucleus accumbens of the rat differentially affects accumbal dopamine release. *Pharmacology & toxicology*, 75, 348-352.

O'Brien, D. P. & White, F. J. (1987). Inhibition of non-dopamine cells in the ventral tegmental area by benzodiazepines: relationship to A10 dopamine cell activity. *European journal of pharmacology*, 142, 343-354.

Oakman, S. A., Faris, P. L., Kerr, P. E., Cozzari, C., & Hartman, B. K. (1995). Distribution of pontomesencephalic cholinergic neurons projecting to substantia nigra differs significantly from those projecting to ventral tegmental area. *The Journal of neuroscience : the official journal of the Society for Neuroscience*, 15, 5859-5869.

Overton, P. G. & Clark, D. (1997). Burst firing in midbrain dopaminergic neurons. *Brain Research Reviews*, 25, 312-334.

Peloquin, J. B., Doering, C. J., Rehak, R., & Mcrory, J. E. (2008). Temperature dependence of Ca-v 1.4 calcium channel gating. *Neuroscience*, 151, 1066-1083.

Pezze, M. A. & Feldon, J. (2004). Mesolimbic dopaminergic pathways in fear conditioning. *Progress in neurobiology*, 74, 301-320.

Picciotto, M. R., Zoli, M., Rimondini, R., Lena, C., Marubio, L. M., Pich, E. M. et al. (1998). Acetylcholine receptors containing the beta2 subunit are involved in the reinforcing properties of nicotine. *Nature*, 391, 173-177.

Pidoplichko, V. I., DeBiasi, M., Williams, J. T., & Dani, J. A. (1997). Nicotine activates and desensitizes midbrain dopamine neurons. *Nature*, 390, 401-404.

Pitts, D. K., Kelland, M. D., Freeman, A. S., & Chiodo, L. A. (1993). Repeated amphetamine administration: role of forebrain in reduced responsiveness of nigrostriatal dopamine neurons to dopamine agonists. *The Journal of pharmacology and experimental therapeutics*, 264, 616-621.

Prisco, S., Natoli, S., Bernardi, G., & Mercuri, N. B. (2002). Group I metabotropic glutamate receptors activate burst firing in rat midbrain dopaminergic neurons. *Neuropharmacology*, 42, 289-296.

Pucak, M. L. & Grace, A. A. (1994). Evidence that systemically administered dopamine antagonists activate dopamine neuron firing primarily by blockade of somatodendritic autoreceptors. *The Journal of pharmacology and experimental therapeutics*, 271, 1181-1192.

Rada, P. V., Mark, G. P., Yeomans, J. J., & Hoebel, B. G. (2000). Acetylcholine release in ventral tegmental area by hypothalamic self-stimulation, eating, and drinking. *Pharmacology, biochemistry, and behavior*, 65, 375-379.

Robbins, T. W. & Everitt, B. J. (1996). Neurobehavioural mechanisms of reward and motivation. *Current opinion in neurobiology*, 6, 228-236.

Robbins, T. W. & Everitt, B. J. (1999). Drug addiction: bad habits add up. *Nature*, 398, 567-570.

Sah, P. (1996). Ca²⁺-activated K⁺ currents in neurones: Types, physiological roles and modulation. *Trends in neurosciences*, 19, 150-154.

Schultz, W. (1998). Predictive reward signal of dopamine neurons. *Journal of neurophysiology*, 80, 1-27.

Schultz, W., Dayan, P., & Montague, P. R. (1997). A neural substrate of prediction and reward. *Science (New York, N.Y.)*, 275, 1593-1599.

Scroggs, R. S., Cardenas, C. G., Whittaker, J. A., & Kitai, S. T. (2001). Muscarine reduces calcium-dependent electrical activity in substantia nigra dopaminergic neurons. *Journal of neurophysiology*, *86*, 2966-2972.

Seeman, P. (1990). Atypical neuroleptics - role of multiple receptors, endogenous dopamine, and receptor linkage. *Acta Psychiatrica Scandinavica*, *82*, 14-20.

Seeman, P., Lee, T., Chau-Wong, M., & Wong, K. (1976). Antipsychotic drug doses and neuroleptic/dopamine receptors. *Nature*, *261*, 717-719.

Seutin, V., Johnson, S. W., & North, R. A. (1993). Apamin increases NMDA-induced burst-firing of rat mesencephalic dopamine neurons. *Brain research*, *630*, 341-344.

Shepard, P. D. & Bunney, B. S. (1988). Effects of apamin on the discharge properties of putative dopamine-containing neurons invitro. *Brain research*, *463*, 380-384.

Shi, W. X. (2009). Electrophysiological characteristics of dopamine neurons: a 35-year update. *Journal of neural transmission.Supplementum*, (73), 103-119.

Smith, J. S., Iannotti, C. A., Dargis, P., Christian, E. P., & Aiyar, J. (2001). Differential expression of KCNQ2 splice variants: Implications to M current function during neuronal development. *Journal of Neuroscience*, *21*, 1096-1103.

Sorenson, E. M., Shiroyama, T., & Kitai, S. T. (1998). Postsynaptic nicotinic receptors on dopaminergic neurons in the substantia nigra pars compacta of the rat. *Neuroscience*, *87*, 659-673.

Steffensen, S. C., Svingos, A. L., Pickel, V. M., & Henriksen, S. J. (1998). Electrophysiological characterization of GABAergic neurons in the ventral tegmental area. *The Journal of neuroscience : the official journal of the Society for Neuroscience*, *18*, 8003-8015.

Stobbs, S. H., Ohran, A. J., Lassen, M. B., Allison, D. W., Brown, J. E., & Steffensen, S. C. (2004). Ethanol suppression of ventral tegmental area GABA neuron electrical transmission involves N-methyl-D-aspartate receptors. *Journal of Pharmacology and Experimental Therapeutics*, *311*, 282-289.

Striessnig, J., Koschak, A., Sinnegger-Brauns, M. J., Hetzenauer, A., Nguyen, N. K., Busquet, P. et al. (2006). Role of voltage-gated L-type Ca²⁺ channel isoforms for brain function. *Biochemical Society transactions*, *34*, 903-909.

Suaud-Chagny, M. F., Chergui, K., Chouvet, G., & Gonon, F. (1992). Relationship between dopamine release in the rat nucleus accumbens and the discharge activity of dopaminergic neurons during local in vivo application of amino acids in the ventral tegmental area. *Neuroscience*, *49*, 63-72.

Takada, M., Kang, Y., & Imanishi, M. (2001). Immunohistochemical localization of voltage-gated calcium channels in substantia nigra dopamine neurons. *The European journal of neuroscience*, *13*, 757-762.

Taylor, L. A. & Creese, I. (2002). Dopamine. In V.S.R.Editor-in-Chief: (Ed.), *Encyclopedia of the Human Brain* (pp. 115-122). New York: Academic Press.

Thierry, A. M., Stinus, L., Blanc, G., & Glowinski, J. (1973). Some Evidence for Existence of Dopaminergic Neurons in Rat Cortex. *Brain research*, *50*, 230-234.

Tong, Z. Y., Overton, P. G., & Clark, D. (1996). Stimulation of the prefrontal cortex in the rat induces patterns of activity in midbrain dopaminergic neurons which resemble natural burst events. *Synapse (New York, N.Y.)*, *22*, 195-208.

Tsuji, M., Nakagawa, Y., Ishibashi, Y., Yoshii, T., Takashima, T., Shimada, M. et al. (1996). Activation of ventral tegmental GABAB receptors inhibits morphine-induced place preference in rats. *European journal of pharmacology*, *313*, 169-173.

Vallone, D., Picetti, R., & Borrelli, E. (2000). Structure and function of dopamine receptors. *Neuroscience and biobehavioral reviews*, *24*, 125-132.

Vargas, G. & Lucero, M. T. (1999). Dopamine modulates inwardly rectifying hyperpolarization-activated current (I_h) in cultured rat olfactory receptor neurons. *Journal of neurophysiology*, *81*, 149-158.

Wahl-Schott, C. & Biel, M. (2009). HCN channels: Structure, cellular regulation and physiological function. *Cellular and Molecular Life Sciences*, 66, 470-494.

Walker, D. & De Waard, M. (1998). Subunit interaction sites in voltage-dependent Ca²⁺ channels: role in channel function. *Trends in neurosciences*, 21, 148-154.

Wang, T. & French, E. D. (1993a). Electrophysiological evidence for the existence of NMDA and non-NMDA receptors on rat ventral tegmental dopamine neurons. *Synapse (New York, N.Y.)*, 13, 270-277.

Wang, T. & French, E. D. (1993b). L-glutamate excitation of A10 dopamine neurons is preferentially mediated by activation of NMDA receptors: extra- and intracellular electrophysiological studies in brain slices. *Brain research*, 627, 299-306.

Waroux, O., Massotte, L., Alleva, L., Graulich, A., Thomas, E., Liegeois, J. F. et al. (2005). SK channels control the firing pattern of midbrain dopaminergic neurons in vivo. *European Journal of Neuroscience*, 22, 3111-3121.

Waszczak, B. L. & Walters, J. R. (1980). Intravenous GABA agonist administration stimulates firing of A10 dopaminergic neurons. *European journal of pharmacology*, 66, 141-144.

Weber, Y. G., Geiger, J., Kampchen, K., Landwehrmeyer, B., Sommer, C., & Lerche, H. (2006). Immunohistochemical analysis of KCNQ2 potassium channels in adult and developing mouse brain. *Brain research*, 1077, 1-6.

Westenbroek, R. E., Hell, J. W., Warner, C., Dubel, S. J., Snutch, T. P., & Catterall, W. A. (1992). Biochemical-properties and subcellular-distribution of an n-type calcium channel-alpha-1 subunit. *Neuron*, *9*, 1099-1115.

White, F. J. (2002). A behavioral/systems approach to the neuroscience of drug addiction. *Journal of Neuroscience*, *22*, 3303-3305.

White, F. J. & Wang, R. Y. (1984). Pharmacological characterization of dopamine autoreceptors in the rat ventral tegmental area: microiontophoretic studies. *The Journal of pharmacology and experimental therapeutics*, *231*, 275-280.

Williams, J. & Lacey, M. (1988). Actions of cocaine on central monoamine neurons: intracellular recordings in vitro. *NIDA research monograph*, *90*, 234-242.

Wise, R. A. (2002). Brain reward circuitry: Insights from unsensed incentives. *Neuron*, *36*, 229-240.

Woolf, N. J. & Butcher, L. L. (1989). Cholinergic systems in the rat brain: IV. Descending projections of the pontomesencephalic tegmentum. *Brain research bulletin*, *23*, 519-540.

Wu, Y. N., Shen, K. Z., & Johnson, S. W. (1999). Presynaptic inhibition preferentially reduces in NMDA receptor-mediated component of transmission in rat midbrain dopamine neurons. *British journal of pharmacology*, *127*, 1422-1430.

Xu, W. F. & Lipscombe, D. (2001). Neuronal Ca(v)1.3 alpha(1) L-type channels activate at relatively hyperpolarized membrane potentials and are incompletely inhibited by dihydropyridines. *Journal of Neuroscience*, 21, 5944-5951.

Yamaguchi, T., Sheen, W., & Morales, M. (2007). Glutamatergic neurons are present in the rat ventral tegmental area. *The European journal of neuroscience*, 25, 106-118.

Yim, C. Y. & Mogenson, G. J. (1980). Electro-Physiological Studies of Neurons in the Ventral Tegmental Area of Tsai. *Brain research*, 181, 301-313.

Yue, C. Y. & Yaari, Y. (2004). KCNQ/M channels control spike afterdepolarization and burst generation in hippocampal neurons. *Journal of Neuroscience*, 24, 4614-4624.

Zhang, J., Chiodo, L. A., & Freeman, A. S. (1994). Influence of excitatory amino acid receptor subtypes on the electrophysiological activity of dopaminergic and nondopaminergic neurons in rat substantia nigra. *The Journal of pharmacology and experimental therapeutics*, 269, 313-321.

Zhang, L., Liu, Y., & Chen, X. (2005). Carbachol induces burst firing of dopamine cells in the ventral tegmental area by promoting calcium entry through L-type channels in the rat. *The Journal of physiology*, 568, 469-481.

Zhang, T. A., Placzek, A. N., & Dani, J. A. (2010). In vitro identification and electrophysiological characterization of dopamine neurons in the ventral tegmental area. *Neuropharmacology*, *59*, 431-436.

Zheng, F. & Johnson, S. W. (2002). Group I metabotropic glutamate receptor-mediated enhancement of dopamine cell burst firing in rat ventral tegmental area in vitro. *Brain research*, *948*, 171-174.

Zhou, Q. Y., Grandy, D. K., Thambi, L., Kushner, J. A., Vantol, H. H. M., Cone, R. et al. (1990). Cloning and expression of human and rat D1 dopamine-receptors. *Nature*, *347*, 76-80.

Zhou, Q. Y. & Palmiter, R. D. (1995). Dopamine-deficient mice are severely hypoactive, adipsic, and aphagic. *Cell*, *83*, 1197-1209.

